City and Environment Interactions 31 (2026) 100407

Contents lists available at ScienceDirect

City and Environment Interactions

journal homepage: www.sciencedirect.com/journal/city-and-environment-interactions

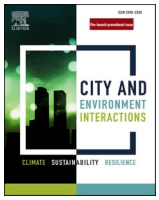

Quantifying the benefits of parks for mitigating heat, air and noise pollution to inform climate-resilient planning

Soheila Khalili [a,b], Laurence Jones [c], Sebastian Pfautsch [d], Prashant Kumar [a,b,*]

[a] Global Centre for Clean Air Research (GCARE), School of Engineering, Civil and Environmental Engineering, Faculty of Engineering and Physical Sciences, University of Surrey, Guildford GU2 7XH, Surrey, United Kingdom
[b] Institute for Sustainability, University of Surrey, Guildford GU2 7XH, Surrey, United Kingdom
[c] UK Centre for Ecology & Hydrology, Deiniol Road, Bangor LL57 2UW, United Kingdom
[d] Urban Transformations Research Centre, Western Sydney University, Locked Bag 1797, Penrith, NSW 2751, Australia

ARTICLE INFO

Keywords:
Park benefits
Urban green infrastructure
Mobile monitoring
Park cool island effect
Urban microclimate

ABSTRACT

Urban parks play a key role in cooling cities and influencing local air quality by providing areas of reduced exposure to pollution sources, alongside local pollution deposition and dispersion effects. However, contemporary practices in designing and managing parks do not specifically plan for these benefits. The present work examines the role of urban parks in providing cooling, human thermal comfort, and reducing air and noise pollution. Using high-frequency mobile monitoring of meteorological variables, air pollutants, and noise levels during summer, measurements were conducted three times per day (morning, afternoon, and evening) to compare a park with the adjacent built environment. Measurements were supplemented by three stationary monitoring points to compare the effect of grassland and tree shade on human thermal comfort. We found that air temperatures cooled by 0.2 °C for every 100 m distance from the edge toward the centre of the park and more than 0.5 °C warming for every 100 m distance from the edge of the park into the adjacent built-up area, with these trends observed up to 300 m. In the evening, PM_{10} (1.63 μg/m^3), $PM_{2.5}$ (0.17 μg/m^3), and PM_1 (0.2 μg/m^3) concentrations increased per 100 m distance from the park edge into the built-up area. Noise levels declined consistently by 3.4 dB per 100 m from the park edge toward the built-up area. Linear mixed-effects models confirmed that parks consistently reduced air temperature and CO_2 levels compared to built-up areas, with the strongest temporal effects in the afternoon, whereas location effects on PM levels were not statistically significant, though distance-based analyses indicated localised and time dependent gradients. Thermal comfort analysis showed greater reductions in Physiological Equivalent Temperature (PET) and Universal Thermal Climate Index (UTCI) under tree-shaded areas than in grassland, with paired *t*-tests indicating significant differences compared to the built-up area, particularly in the afternoon. Presenting the environmental benefits per unit of distance makes the results presented here relevant for professionals who are interested in developing effective heat-, noise- and pollution-responsive urban landscape design, while indicating spatial variability in air quality responses. Such an evidence-based approach can lead to greater community benefits and thus improved resilience of cities.

1. Introduction

Urbanisation and climate change have created an urgent need for sustainable urban planning strategies that prioritise environmental resilience and the well-being of urban residents [1]. In this context, green infrastructure emerges as a pivotal component of climate-smart urban planning and design [2,3]. Green infrastructure provides ecosystem services that enhance environmental, social, and economic values [4–6]. These services include mitigation of urban overheating, localised carbon dioxide (CO_2) uptake by vegetation, improvements in air and water quality, flood risk reduction, and the provision of recreational and restorative spaces that support public health and well-being [7–9].

Urban parks, as a key component of urban green infrastructure, play

* Corresponding author at: Global Centre for Clean Air Research (GCARE), School of Engineering, Civil and Environmental Engineering, Faculty of Engineering and Physical Sciences, University of Surrey, Guildford GU2 7XH, Surrey, United Kingdom.
E-mail address: p.kumar@surrey.ac.uk (P. Kumar).

https://doi.org/10.1016/j.cacint.2026.100407
Received 31 January 2026; Received in revised form 27 May 2026; Accepted 5 June 2026
Available online 6 June 2026
2590-2520/© 2026 The Authors. Published by Elsevier Ltd. This is an open access article under the CC BY license (http://creativecommons.org/licenses/by/4.0/).

a vital role in regulating the urban microclimate. Through shading and evapotranspiration, parks provide cooling benefits and enhance thermal comfort for users, particularly during the summer season [10–12]. Beyond thermal regulation, urban parks can also influence local air quality by facilitating the dispersion and deposition of pollutants, thereby reducing human exposure to harmful particulates. Furthermore, urban parks serve as critical acoustic buffers; the presence of vegetation, uneven terrain, and soft ground surfaces can significantly attenuate urban noise compared to the reflective surfaces found in densely built environments [13].

A substantial body of previous studies has employed diverse monitoring methodologies to assess the park's environmental benefits in terms of heat mitigation [14–17], air quality improvement [18,19], thermal comfort enhancement [20–23], and noise attenuation [24–26] across various urban contexts and park characteristics (Table 1). Previous research confirms that air and surface temperatures within parks are typically lower than in surrounding built-up areas [27,28], with cooling distances reported to range from tens to several hundreds of metres depending on park size, perimeter complexity, and vegetation cover type, age and quality of plant species and irrigation [29–31]. For instance, satellite-based studies have reported cooling benefits ranging from 100 m to over 150 m for various park sizes [10,28] while field-based studies suggest the cooling effect may extend further, particularly at night [16]. However, this evidence mainly remains centred on cooling benefits, often relying on short-term datasets or spatially coarse indicators such as land surface temperature. As a result, fine-scale spatial gradients that propagate from parks into the adjacent built-up areas have been less discussed.

Beyond the cooling effect, studies assessing the improvement of air pollution and noise reduction by urban parks are comparatively limited and frequently conducted in isolation. As summarised in Table 1, air quality studies mostly focus on pollutant removal efficiency or near-road gradients over short distances [19,35]. Similarly, noise mitigation studies often report average attenuation levels without examining spatial gradient patterns across park-urban interfaces [34,36].

Collectively, these studies highlight the capacity of urban parks to deliver multiple environmental benefits, but they have mainly focused on evaluating single benefits [37,38]. Furthermore, the synergy between cooling benefit and air quality improvement is not static throughout the diurnal cycle, as atmospheric stability and traffic patterns shift throughout a day. Failure to account for these temporal dynamics and potential trade-offs risks oversimplifying the role of urban park interventions. Consequently, a comprehensive integration of multiple benefits using real-time, high-resolution evaluation that simultaneously quantifies how multiple benefits vary with distance from parks remains underexplored. Integrating these measurements can provide insights into spatial gradients and the co-provision of multiple ecosystem services within and around urban parks, thereby supporting the development of planning-relevant guidance for climate-resilient urban design. Furthermore, although mobile monitoring approaches enable a deeper understanding of park benefits extending beyond park boundaries [39,40], their limited application continues to constrain understanding of fine-scale spatial gradients and multi-benefit interactions.

To address this gap, this study employs high-resolution mobile monitoring to quantify the spatial and temporal gradients of multiple environmental benefits provided by an urban park and its surrounding built-up areas. Simultaneous measurements of air temperature, particulate matter (PM_{10}, $PM_{2.5}$, PM_1), carbon dioxide (CO_2), thermal comfort indicators, and noise levels were collected to capture real-time pedestrian-scale exposure under periods of elevated pollution and thermal stress. By integrating microclimate, air quality, thermal comfort, and noise conditions within a single analytical framework, this study provides a comprehensive evaluation of parks' multi-benefits. This approach enables assessment of both the magnitude and spatial extent of park benefits, offering practical insights into how urban parks can simultaneously improve multiple environmental benefits.

The specific objectives of this study are to: (i) compare air quality, microclimate conditions, thermal comfort, and noise conditions between the park and adjacent built-up areas; (ii) quantify distance-based gradients and rates of change in cooling, air pollution, and noise attenuation across the park and built-up area interface, and (iii) how thermal comfort differs between a built-up area and two locations in the park that feature different types of green infrastructures: grassland versus tree-shaded area. In addition, this study explores potential synergies and trade-offs among these environmental benefits by analysing their concurrent spatial patterns. Together, these analyses provide planning-related evidence on the magnitude, spatial gradient, and integration of park-related environmental benefits, supporting climate-resilient urban design and decision-making.

2. Methodology

This study employs a real-time data collection approach to assess the benefits of an urban park during summer in terms of air quality, cooling effects, thermal comfort, and noise levels. The primary environmental variables examined include air temperature, air pollutants (PM_{10}, $PM_{2.5}$ and PM_1), CO_2, thermal comfort indices, specifically Universal Thermal Climate Index (UTCI) and Physiologically Equivalent Temperature (PET), which quantify human thermal stress under outdoor conditions. Sound levels were measured using the A-weighted equivalent continuous sound pressure level (LAeq), calculated as the logarithmic average of all A-weighted sound readings over 30-s intervals (detailed procedure in Section 2.3).

2.1. Study design

This study was designed to evaluate the benefits of a typical urban park, with a particular focus on its role in providing cooling, improving air quality, enhancing thermal comfort, and mitigating noise compared to the surrounding built-up area. A mobile monitoring approach was adopted to capture real-time, high-resolution data across the park and surrounding built-up area, allowing direct comparison between these urban settings.

Measurements were collected over multiple days during morning, afternoon, and evening periods to capture diurnal variation. Data collection was conducted during summer, when heat stress is most pronounced and park use is most frequent, providing a representative context for evaluating park benefits under peak conditions. A fixed route was followed for each monitoring session, covering representative sections of both the urban park and adjacent built-up areas, with five replicate transects running to/from the park to the adjacent urban residential area. The data collection strategy was designed to minimise variability due to external factors and enable consistent spatial and temporal comparison across sites. Further details on the site, instrumentation, data collection protocols, and analytical methods are provided below.

2.2. Site description

The study was conducted through a field campaign in Guildford, UK (Fig. 1). Guildford is located in Surrey County, southeast of the UK (51.215° latitude and − 0.631° longitude) and features a humid temperate oceanic climate (Köppen climate classification: Cfb [41]). The population of Guildford was 151,359 in 2024, with a 6.3% growth over the previous five years [42]. Ambient air temperatures are highest during summer, with July typically the warmest month based on long-term averages, and lowest in January. Mean summer air temperatures are approximately 17.3 °C, while winter averages are around 4.7 °C [43]. During summer 2024, peak hot conditions in south-east England occurred in mid-August, with daily maximum temperatures reaching 35 °C, recorded at the London Heathrow Met Office station, the nearest long-term reference station to Guildford [44]. Fig. 1h presents

Table 1
Past monitoring studies on the assessment of the co-benefits provided by parks.

Benefit	Method	Characteristics	Duration	Location/ climate type	Key Finding	Reference
Heat mitigation	Remote sensing	0.5 to 23.3 ha	Three years	Hangzhou, China- Cfa	Assessed the cooling benefits of twenty newly constructed parks using three years of satellite data. The results revealed that the newly built parks reduced LST by 0.31∘C inside the park and 0.64∘C in the adjacent built-up area, reaching to 0.84∘C and 1.09 ∘C as parks mature, with cooling distance rising from 104.4 m to 147.5 m.	Wu et al. [28]
	Remote sensing	1 to 100 ha	September	Hangzhou, China- Cfa	Assessed cooling performance of 220 parks, finding that 84% exhibited cooling effects with average, maximum, and cumulative cooling intensities of 0.35 °C, 2.35 °C, and 0.05 °C, respectively. Identified significant neighbourhood disparities, with 57% exposed to less than 0.06% cooling. The estimated total carbon savings at approximately 1.13×10^4 t, and the highlighted park perimeter is a key factor influencing cooling outcomes.	Guo et al. [31]
	Remote sensing	Average area 112.57 ha	June to September	Yreb, China- Cwa/Cfa	Reported cumulative cooling intensity and gradient values providing valuable insights into the quantitative aspects of park cooling. The results showed that parks average cooldown LST by 2.34 ± 0.07∘C, 151.43 ± 4.39 m.	Shi et al. [10]
	Fixed and mobile monitoring	52 ha	Whole year	Guildford, UK- Cfb	Evaluated the cooling benefit of various GI types, including parks, during a year. The results showed that the daytime air temperature was lower in the park by up to 3∘C, and up to 1.5∘C at nighttime.	Sahani et al. [8]
	Remote sensing	Area varies from 1.1 to 281.6 ha, with an average of 24.3 ha	One day (September)	Liuzhou, China- Cfa/Cwa	Explored park cooling performance based on LST, highlighting that the urban park exhibited an average cooling distance of 166.17 ± 11.69 m and a cooling intensity of 2.85 ± 0.28 °C, covering about five times the park area.	Shi et al. [11]
	Fixed and mobile monitoring	Area varies from 15.21 to 285.25 ha	July and August	Beijing, China - Dwa	Investigated the impact of large urban parks on the local climate in Beijing. The results showed that during summer nights, parks reduced night-time air temperatures, with their cooling effect extending over 1 km, with more effective cooling effects within approximately one park width.	Li et al. [16]
	Fixed and mobile monitoring	Covered with an open lawn (30%) and forest canopy (60%).	Seven days of mobile and two months of fixed monitoring	Tokyo, Japan- Cfa	Contributed insights into the vertical profiles of air temperature in park and town areas, measuring a cold air pool in the park's first 50 m from the ground, as opposed to neutral stratification in the town area.	Sugawara et al. [17]
Thermal comfort	Field measurement and questionnaire survey	Park area: 125 ha	Over six summer days at two-week intervals	Madrid, Spain- Csa	Revealed that the park's cooling effect extended up to 600 m outward from the park boundary, lowering maximum air temperature by 2.4–2.8 °C and reducing the PET by approximately 3.9 °C.	Aram et al.[32]
Air pollution improvement	Field measurement	Park area varied from 0.65 to 3.96 ha	During spring	Hong Kong- Cwa	Demonstrated a swift decline in pollutant concentrations downwind from the roadside, stabilising within tens of metres, while an even more pronounced gradient was observed upwind, with a rapid increase detected within 2 m of the road edge.	Xing and Brimblecombe [19]
	Field measurement	Over 80% of the area is covered by vegetation	Four months (January, April, July, and October)	Shanghai, China- Cfa	Indicated that park vegetation removed 9.1% of total suspended particulates, 5.3% of SO2, and 2.6% of NO_2. In addition, the crown volume coverage and pollution diffusion distance were pivotal predictors influencing the rate of pollutant removal.	Yin et al. [33]
Co-benefits in terms of air pollution	Field measurement	Park area: 2.8 ha, containing mature trees,	Eight days (four days in summer	Tel-Aviv, Israel- Csa	Urban parks were found to lower NO_x, CO, and PM_{10} levels while increasing O_3	Cohen et al. [34]

(continued on next page)

Table 1 (*continued*)

Benefit	Method	Characteristics	Duration	Location/ climate type	Key Finding	Reference
improvement and noise mitigation		bushes, and lawn, with 85% tree coverage.	and four days in winter)		concentrations, with a more substantial mitigation effect observed at higher levels of NO_x and PM_{10}. Additionally, parks can reduce noise by ~approximately 5 dB(A).	

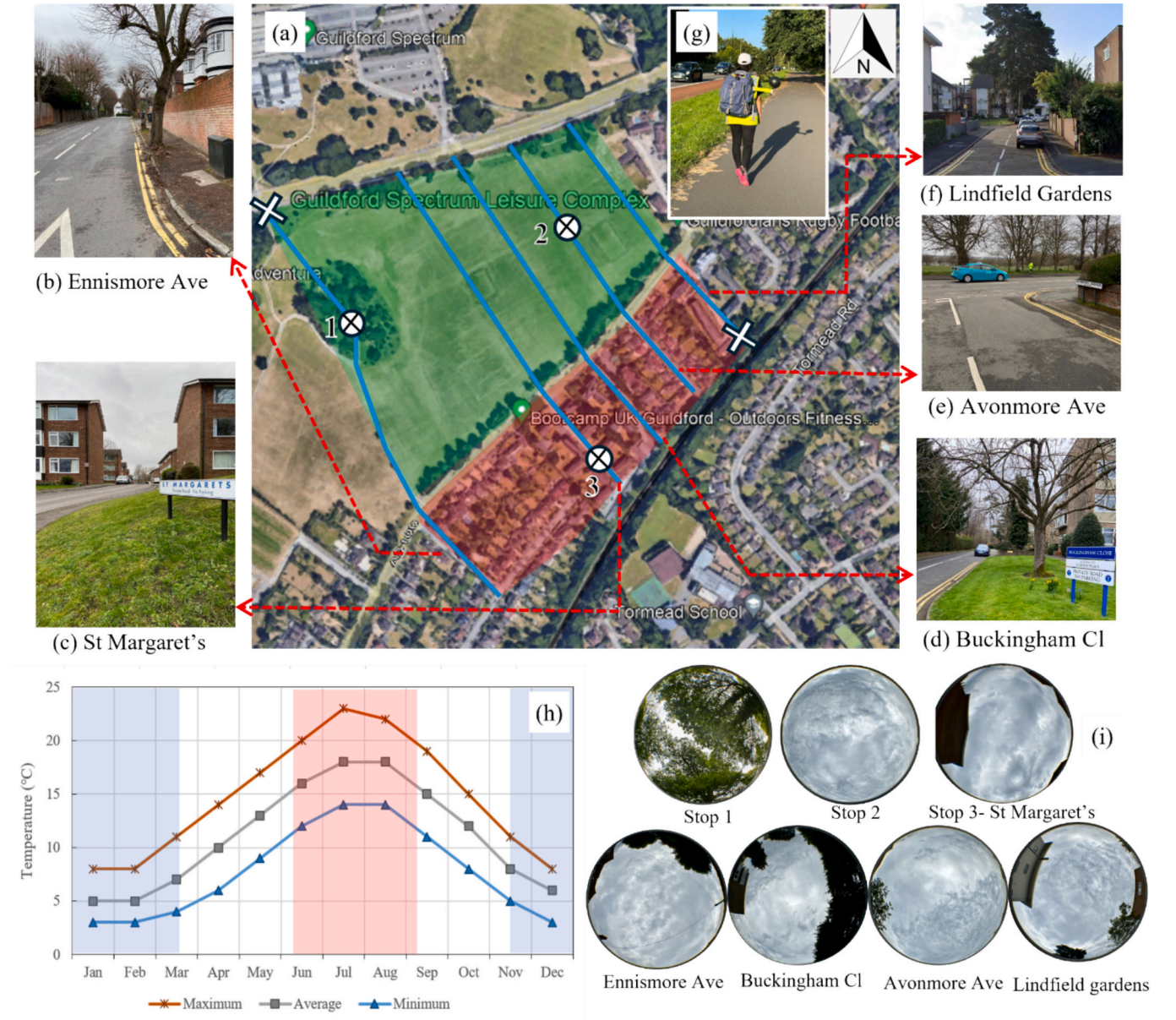

Fig. 1. (a) Location and the path for mobile monitoring of meteorological parameters, showing the five replicate transects. The 'x' marks start and end points of the walking route and white-crossed circles show the stops in (1) the tree-shaded area, (2) the grassland, and (3) the built-up area. Panels (b) to (f) show the surrounding streets and the built-up area. Panel (g) illustrates the mobile sensor backpack and researcher. Panel (h) depicts average monthly minimum, mean, and maximum air temperatures in Guildford (Source: [45]), ranging between 5 °C and 18 °C. Fisheye lens images (i) show the sky view at each of the three stationary monitoring points and adjacent streets.

the monthly minimum/ mean/ maximum air temperature in Guildford, UK.

The site chosen for monitoring was Stoke Park, the largest and most popular park in the centre of Guildford, with 50 ha of grasslands, gardens, and trees, and the surrounding built-up area (Fig. 1a–f). Yellow lines in Fig. 1a depict the mobile monitoring path across the park and the surrounding built-up area. This study route was designed to evaluate potential spatial variation in air temperature, thermal comfort conditions, air quality, and noise levels between the park and the adjacent built-up residential area. The built-up area adjacent to the park consists

primarily of residential streets with an average width of 9 m, lined with buildings typically one to two stories high, and a surface composition that includes asphalt, paving, and some vegetation. The park itself includes a combination of open grassland and tree-shaded areas. The internal transects within the park extended up to 240 m from the park edge toward the centre, while the transect into the built-up area reached distances of up to 300 m from the park boundary. This extent was selected to capture the transition zone where the most pronounced changes in microclimatic conditions are expected, consistent with previous studies reporting sharp gradients in temperature and air quality within a few hundred metres of park boundaries [46–48].

These distances define the spatial extent used to assess rates of change in environmental parameters. Sky view factor (SVF) is defined as the fraction of the sky hemisphere visible from a point on the ground, ranging from 0 (completely obstructed) to 1 (fully open) [49]. It is calculated by integrating visible sky angles over the hemisphere, typically using fisheye photography [50]. In this study, SVF values ranged from 0.46 to 0.69 in the built-up area and from 0.20 to 1 in the park, with values approaching 1 measured in large open grassland areas where trees or buildings at the park perimeter did not obstruct the local sky view.

The topography of the study area is relatively flat with an elevation change of approximately 6.5 m between the centre of the park and the end point of the transect in the residential neighbourhood. The three stationary monitoring points represented distinct microenvironments (Fig. 1a): Stop 1 was positioned in a tree-shaded area with a SVF of 0.20 and located 217 m from the built-up area; Stop 2 was placed in open grassland with minimal shade or impervious surface influence (SVF, 1); and Stop 3 was in a built-up street canyon, surrounded by hard surfaces and limited vegetation cover (SVF, 0.61). Thermal comfort was assessed at the three stationary monitoring points, selected to represent the principal microenvironments within the study area: grassland, tree-shaded, and built-up settings. These points capture the range of thermal conditions typically experienced by park users and provide a basis for comparing landscape types.

Five mobile transects were conducted across different sections of the park and adjacent built-up residential areas to ensure spatial representativeness. Detailed descriptions of transect routes and sequences are provided in the Supplementary Materials (Text S1).

2.3. Instrumentation

A bespoke integrated monitoring system was prepared to house various instruments in a backpack (Fig. 1g) to measure air temperature (T_a), relative humidity (RH), wind speed (v), black globe temperature (T_g), CO_2, PM_{10}, $PM_{2.5}$, PM_1, and sound levels alongside a GPS device to map the exact location and time of each observation. The same set of instruments was used at the three stationary monitoring points to ensure data comparability across locations.

Meteorological parameters and CO_2 levels were recorded using the Testo 400 multifunctional environmental meter. The Testo 400 is widely used in outdoor studies for its accuracy and portability [51–53]. PM concentrations (PM_{10}, $PM_{2.5}$, and PM_1) were measured using the GRIMM 11D aerosol spectrometer (GRIMM Aerosol Technik GmbH & Co KG, Ainring, Germany). Detailed probe specifications and measurement ranges are provided in the Supplementary Materials (Text S2). PM data were recorded every 6 s, offering detailed insights into temporal variations in particulate levels. Ambient sound levels were monitored using a calibrated sound level meter (RS PRO 1151), which recorded A-weighted sound pressure levels (dB) every second, within a range of 30 to 110 dB and with a resolution of 0.1 dB. A GPS device (GARMIN ETREX 32×) was used to capture geospatial coordinates and synchronise time across datasets. The average A-weighted equivalent sound pressure level for over 30 s ($LAeq_{30sec}$) is calculated using Eq. (1) [54], where Li represents each sound pressure level reading in dB and n is the total number of measurements. Similar short-term time averages have been used in previous studies [55–57].

$$LAeq = 10log\frac{1}{n}\sum_{i=1}^{n}10^{Li/10} \quad (1)$$

2.4. Data collection

The data for this study were collected while walking along several defined transects (Fig. 1a). Each of ten data collection campaigns (15 August 2023–5 September 2023) consisted of three-time intervals (morning: 8:00–9:00, afternoon: 12:30–13:30, evening: 17:00–18:00). These periods were chosen to capture peak traffic and to sample temperatures approaching the daily maximum, which typically occurs early to mid-afternoon. During the monitoring period, daily maximum air temperatures ranged approximately between 20 °C and 30 °C, with peak values exceeding 30 °C following the mid-August heatwave; conditions were predominantly clear to partly cloudy, rainfall was intermittent (<5 mm day^{-1}), and mean wind speeds were generally below 5 m/s. The prevailing wind direction during the monitoring sessions was from the west [58]. The 4-km route was walked at a normal pace while carrying a backpack-mounted sensor system (Fig. 1g), with probes positioned at 1.4–1.7 m height (approximating head level for a 1.6–1.8 m tall person). The main sensors extended to ear height (~1.5 m), while the black globe thermometer was placed 10 cm lower (~1.4 m) to avoid backpack frame interference. Temperature and radiation probes were mounted on rigid 40 cm extension arms to prevent body shading, and the backpack design incorporated mesh panels to ensure adequate ventilation around all sensors (Fig. 1g). A summary of the mobile monitoring sessions, including the route direction, average duration, and the number of data points collected for each parameter on different dates and times of day, is provided in Table S1.

2.5. Data analysis

Data analysis was done using RStudio (V4.2.2), Microsoft Excel, QGIS (V4.0.0), and RaymanPro to evaluate spatio-temporal variations in microclimatic, air quality, and noise level parameters, and to assess thermal comfort conditions. To evaluate the effect of location type (park versus built-up area) and time of day (morning, afternoon, evening), Linear Mixed Effects Models (LMM) were used. Linear regression models were used to describe the continuous relationship between environmental variables and distance along the measurement path, providing a quantitative assessment of spatial gradients. Statistical significance was evaluated using p-values with a threshold of $p < 0.05$ considered significant.

For distance-based analysis, a moving-average smoothing method was applied to reduce short-term variability and highlight spatial trends along the transects. Temporal variability during mobile monitoring was addressed by (i) conducting measurements within relatively short time windows (≤60 min), (ii) repeating transects across multiple days and times of day, and (iii) applying moving-average smoothing in the distance-based analysis to reduce short-term temporal noise and emphasise spatial patterns. Under the relatively stable meteorological conditions observed during the monitoring period (predominantly clear to partly cloudy conditions and moderate winds), temporal changes in background conditions are expected to be gradual compared to the spatial contrasts captured along the transects. The window size—the number of consecutive data points averaged—was selected to provide a consistent smoothing duration of approximately 12 s (12 points for 1-s data; 2 points for 6-s data), balancing noise reduction with preservation of spatial resolution, in line with previous mobile monitoring studies using similar moving average intervals to reduce short-term variability while maintaining spatial fidelity [59,60].

QGIS was used to generate spatial maps and visualise gradients in microclimatic parameters and pollutant concentrations along the mobile monitoring transects. It was also used to map each value's location type

(park or built-up area) using GPS coordinates. The spatial gradients enabled comparison between the park and the built-up area. To visualise the spatial gradient of variables, raw point data from the validated monitoring days were integrated using a Spatial Join (Summary) technique in QGIS 4.0.0. The study area was divided into a 20-m hexagonal grid (tessellation). This 20 m resolution was chosen to balance GPS accuracy. For each hexagonal cell, the arithmetic mean of all contained data points across the multi-day period was calculated. To minimise the influence of transient conditions, days where the diurnal median of a variable exceeded two standard deviations from the study period mean were excluded. Additionally, hexagonal cells containing fewer than three data points were removed. This spatial binning approach minimises the impact of GPS drift and transient pollutant pulses, highlighting persistent hotspots where concentrations were consistently elevated across the monitoring period.

Environmental gradients derived from the distance-based analysis were synthesised to quantify synergies and trade-offs among cooling and air-quality benefits. To ensure comparability across parameters recorded at different temporal resolutions and to avoid bias arising from bidirectional walking transects, all measurements were aggregated into fixed 10 m distance bins prior to analysis. Synergies and trade-offs were quantified using an Exposure-Adjusted Synergy Index (EASI), with air temperature used as the reference service:

$$EASI_{T,X} = sign(\beta_T^*).sign(\beta_X^*).min\left(\frac{|\beta_X|}{|\beta_T|}, 1\right) \quad (2)$$

where β_T and β_X represent the spatial rates of change of air temperature and variable X (e.g., relative humidity, CO_2, PM_{10}, $PM_{2.5}$, PM_1) with distance from the park. Positive EASI values indicate synergistic responses, where changes in X align with the thermal gradient, while negative values indicate trade-offs, where changes in X oppose the thermal gradient. Analyses were conducted separately for park and built-up areas and stratified by time of day (details are provided in SI Text S3).

The SVF was calculated using a custom Python script implemented via Google Drive to process fisheye images, providing essential input for subsequent thermal comfort assessment. Thermal comfort was assessed using the PET and UTCI indices, calculated with RaymanPro, which integrates air temperature, humidity, wind speed, and radiation to quantify human thermal comfort conditions. Both indices were applied to provide a robust characterisation of outdoor thermal conditions and were selected due to their extensive validation under outdoor conditions and suitability for comparative analysis [61–63].

The PET is a widely used thermal comfort index that estimates the equivalent temperature at which a person would feel the same thermal sensation in a standard indoor environment. The human energy budget for the assumed condition is balanced by the same sweat rate and skin temperature as under the actual outdoor conditions to be assessed [64]. The calculation of PET relies on advanced numerical models, such as the Munich Energy-balance Model for Individuals and software like Rayman. These tools simulate human energy balance and the heat exchange processes occurring in outdoor environments, ultimately providing a temperature equivalent expressed in degrees Celsius (°C) to assess thermal comfort. The PET categorises thermal comfort conditions as follows: below 18 °C indicates "slightly cool" to "cold" conditions; between 18 and 23 °C is considered as thermally comfortable; between 23 °C and 29 °C reflects "slightly warm"; and values exceeding 29 °C suggest increasing levels of discomfort. This classification is consistent with regional evidence: a study in Cambridge, UK, reported a summer neutral PET of approximately 21 °C [65], supporting the selection of 18–23 °C as an appropriate comfort range for interpreting thermal perceptions in Guildford.

The UTCI integrates air temperature, wind speed, humidity, and radiation to provide a comprehensive measure of thermal stress experienced by individuals in outdoor environments. It is expressed in °C and is widely used to assess the impact of heat on human health and comfort. The UTCI is calculated through a multi-step process, using Eq. (3):

$$UTCI = f^{-1}[(T_a, T_m, v_a, RH, M)] \quad (3)$$

In Eq. (2), T_a represents the air temperature in °C, and T_m refers to the mean radiant temperature in °C. The variable v_a is the wind speed at a height of 10 m, expressed in metres per second (m/s), RH represents the relative humidity (%), and M is the metabolic rate in watts per square meter (W/m^2), which accounts for the level of physical activity of the individuals. Higher levels of physical activity increase metabolic heat production, which can elevate thermal stress and reduce perceived thermal comfort [66]. UTCI categorises thermal comfort conditions as follows: below 9 °C indicates cold stress, between 9 °C and 26 °C represents "no thermal stress", and values above 26 °C reflect moderate to strong heat stress. These indices were used to quantify and compare thermal comfort conditions across different urban settings.

3. Results

The result section begins with a detailed overview of air quality and microclimate parameters, including their distribution patterns. This is followed by statistical testing using LMM to examine the effects of location and time of day on these variables. Next, temporal variations are explored through daily and location-based trends to understand changes over time. Spatial gradients are then analysed to assess how environmental conditions differ between the park and the surrounding built-up area. A distance-based analysis quantifies the rate at which air temperature and pollutant levels change moving away from the park boundary. Finally, the study investigates additional benefits of the park, focusing on its role in enhancing thermal comfort and mitigating urban noise.

3.1. Overview of air quality and microclimate parameters

Fig. 2 presents the variation in air temperature, relative humidity, CO_2, PM_{10}, $PM_{2.5}$, and PM_1 concentrations comparing the park with surrounding built-up areas during morning, afternoon, and evening measurement periods, with complete descriptive statistics available in Table S2. The analysis indicates a consistent difference between the park and built-up areas.

The average air temperature in the park was 18.5 °C in the morning and 25.7 °C in the afternoon, compared with 19.8 °C and 27.0 °C, respectively, in the built-up area. This corresponds to a 1.3 °C reduction in morning and afternoon temperatures within the park. In the evening, the park was slightly cooler than the built-up area, with temperatures of 23.0 °C compared with 24.0 °C, corresponding to a 1 °C reduction. The LMM analysis (Section 3.1.2) confirmed that location (park vs. built-up area) significantly influenced air temperature.

Relative humidity was generally higher in the park, especially in the afternoon and evening. However, the LMM analysis indicated that the effect of location was not statistically significant ($p = 0.71$; Section 3.1.2). Although overall spatial differences were limited, clear temporal variations were evident across the measurement periods.

CO_2 concentrations were consistently lower in the park compared to the surrounding built-up areas. The LMM analysis confirmed that this difference by location was statistically significant (Section 3.1.2). CO_2 reductions of 2.3–3.3% were observed in the park during morning and afternoon periods. In contrast, while PM_{10}, $PM_{2.5}$, and PM_1 concentrations were generally lower in the park across all time periods, these variations did not reach statistical significance according to the LMM results (Section 3.1.2). Despite the lack of statistical significance, the descriptive data showed that the largest mean reductions occurred in the morning, at 11.6%, 10.9%, and 4.2% for PM_{10}, $PM_{2.5}$, and PM_1, respectively, while afternoon and evening mean decreases ranged from 0.9% to 4.8%.

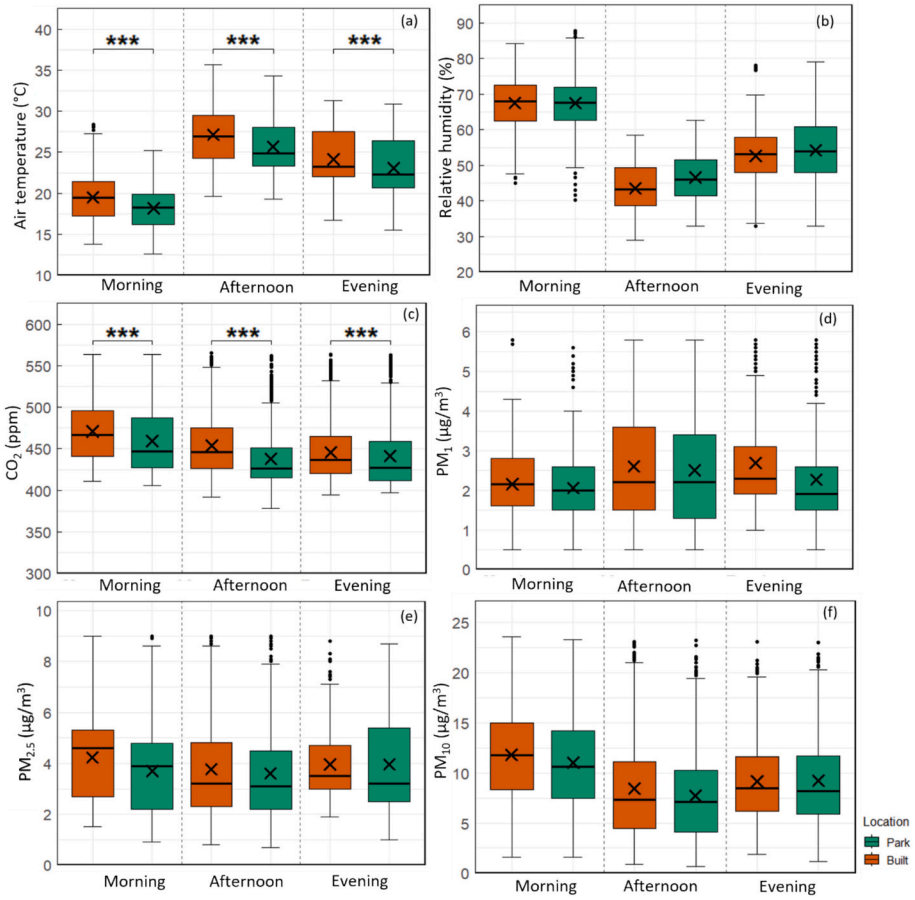

Fig. 2. (a) Air temperature, (b) relative humidity, (c) CO_2, (d) PM_1, (e) $PM_{2.5}$, and (f) PM_{10} data boxplots depiction featuring the median (thick horizontal black line), mean (cross) measured during morning, afternoon, and evening runs at the built-up area and the park. Statistical significance was determined via Linear Mixed Model analysis; brackets with asterisks (***, $p < 0.001$) denote significant differences between the built-up area and the park locations, while the absence of brackets indicates no statistically significant difference ($p > 0.05$).

3.1.1. Density distributions of air quality and microclimate parameters

While the previous section highlighted average reductions in temperature and pollution in the park, the density plots (Fig. 3) offer deeper insight into the distribution and variability of these parameters. The built-up area generally shows distributions shifted toward higher values for air temperature, particularly in the afternoon, indicating higher and more variable conditions. The park, by contrast, maintains lower-temperature distributions, reflecting cooler and more stable microclimates. Relative humidity is consistently higher in the park, especially in the morning and evening.

CO_2 and PM levels also tend to be shifted toward higher concentrations in the built-up area, suggesting greater emissions and variability, while pollutant distributions in the park are lower and more concentrated, indicating reduced pollution levels. These patterns show that the park not only reduces average levels but also helps maintain a more consistent environment across the day and overall stability of the park environment.

3.1.2. Linear mixed effects models on microclimate and pollutants variables

To investigate how environmental conditions vary across locations and time, LMMs were applied to each microclimatic and air quality parameter. While the previous section presented descriptive distribution patterns, the statistical significance of these differences between park and built-up areas is evaluated in this section using the LMM method. This analysis assessed the effects of location (park vs. built-up area), time of day (morning, afternoon, evening), and their interaction, while accounting for repeated measurements and random variability across sampling days. The models provided insight into the relative contributions of spatial and temporal factors to observed patterns in air temperature, relative humidity, CO_2, and PM concentrations, with results summarised in Table 2.

Air Temperature exhibited significant differences between locations, with the park location consistently cooler than the built-up area (estimate = −1.89, $p < 0.001$). Time of day strongly affected temperature, increasing in the afternoon (estimate = 7.58, $p < 0.001$) and evening (estimate = 4.92, $p < 0.001$) relative to morning. Interaction effects between location and time were not statistically significant (Park: Afternoon, $p = 0.16$, Park: Evening, $p = 0.05$), indicating consistent diurnal temperature patterns across environments. These findings confirm that parks have a thermal regulation effect, maintaining cooler air temperatures relative to built-up areas throughout the day, with an absolute temperature difference of approximately 1.89 °C. Relative Humidity was primarily influenced by time of day, declining markedly in the afternoon (estimate = −24.46, $p < 0.001$) and evening (estimate = −15.84, $p < 0.001$). No significant differences were observed between locations ($p = 0.710$), nor were interaction effects significant (Park: Afternoon, $p = 0.12$, Park: Evening, $p = 0.52$), suggesting similar temporal humidity dynamics in both settings. CO_2 concentrations varied significantly by location ($p < 0.001$) and time of day, with concentrations decreasing through the afternoon and evening ($p < 0.001$). The average CO_2 concentration was higher in the built-up area compared to the park.

For PM levels, temporal effects were observed, with significantly lower concentrations observed in the afternoon and evening compared to morning (all $p < 0.001$). Location effects were not statistically significant for PM_1 ($p = 0.35$), $PM_{2.5}$ ($p = 0.07$), or PM_{10} ($p = 0.20$),

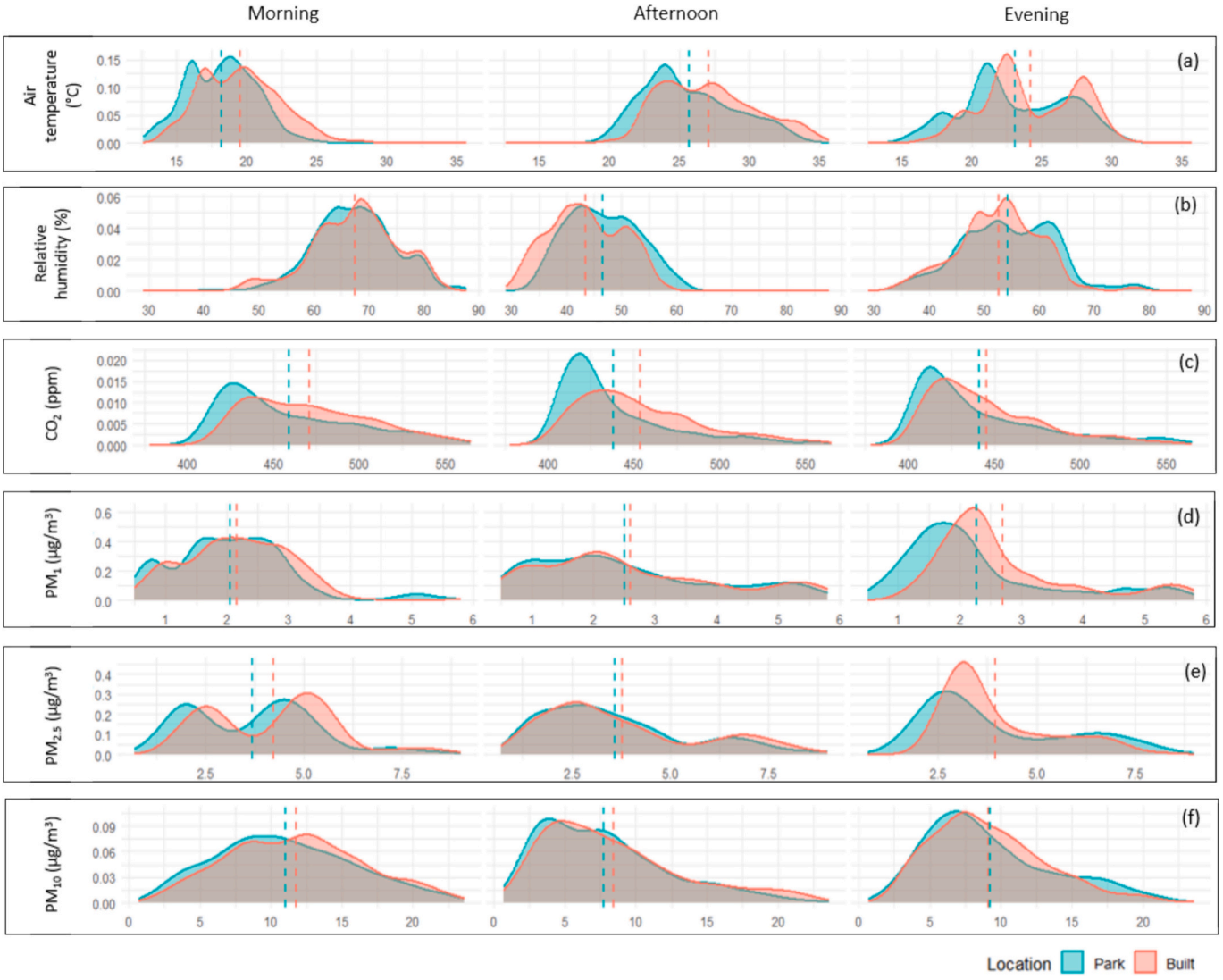

Fig. 3. Density plots of (a) Air Temperature, (b) Relative Humidity, (c) CO_2, (d) PM_1, (e) $PM_{2.5}$, and (f) PM_{10} measured in park and built-up areas across different times of day (Morning, Afternoon, Evening). Each plot shows the distribution of values by location, with dashed vertical lines indicating mean values.

indicating no clear difference in PM concentrations between park and built-up areas, and no significant interaction terms were detected.

Overall, these findings demonstrate that while microclimatic variables and CO_2 exhibit significant spatial and temporal variability, PM concentrations are predominantly modulated by time of day. The absence of significant interaction effects across PM concentrations implies consistent diurnal patterns in both park and built-up areas. In summary, the findings reveal that both location and time of day significantly influence microclimatic and air pollutant levels, while interaction effects between location and time of day were not statistically significant.

3.2. *Temporal variation of air quality and microclimate parameters*

To assess temporal variability in environmental conditions, daily mean values of air temperature, relative humidity, CO_2, PM_{10}, $PM_{2.5}$, and PM_1 were summarised separately for the park and the built-up area. Across all measurement days, mean air temperature in the park ranged from 17.9 °C to 25.2 °C, relative humidity from 49.8% to 61.5%, and CO_2 concentrations from 429 to486 ppm. Mean concentrations of PM_1, $PM_{2.5}$, and PM_{10} in the park ranged from 0.96 to 5.54 µg/m^3, 1.85 to 7.39 µg/m^3, and 6.42 to 15.6 µg/m^3, respectively. Across the same period, mean air temperature in the built-up area ranged from 19.3 to 28.8 °C, relative humidity from 49.4 to 58.3%, and CO_2 concentrations from 443 to 511 ppm. PM_1, $PM_{2.5}$, and PM_{10} concentrations in the built-up area ranged from 1.25 to 6.01 µg/m^3, 2.33 to 7.21 µg/m^3, and 7.36 to 17.0 µg/m^3, respectively. Fig. S1 presents the daily mean values for each parameter, with paired data points for the park and built-up area connected by lines to illustrate temporal variation across the monitoring period.

Time series plots were used to examine changes in microclimate and air quality within each 60-min monitoring session, separately for the park and the built-up area, during morning, afternoon, and evening periods. These plots display the progression of air temperature, relative humidity, CO_2, and PM levels along the traversed path (Fig. 4).

Minute-by-minute trends reveal intra-period variation, showing that the built-up area consistently experienced higher temperatures and pollutant concentrations. Temperature differences peaked in the afternoon, whereas pollutant contrasts were greatest during the morning traffic period.

Table 2
Results of Linear Mixed Effect Model testing the effects of location (park versus built-up area) and time of day (morning, afternoon, evening) on microclimate variables (air temperature, relative humidity, CO_2) and PM concentrations (PM_1, $PM_{2.5}$, PM_{10}). The table summarises degrees of freedom (df), t values, p-values, and the significance of main effects and interactions.

Parameter	Term	Estimate[a]	Std. Error	df[b]	t value	*p*-value	Significance
Air temperature (°C)	Intercept	19.44	0.92	11.14	21.24	<0.001	✓
	Location (Park)	−1.89	0.44	263.15	−4.28	<0.001	✓
	Time (Afternoon)	7.58	0.43	263.34	17.46	<0.001	✓
	Time (Evening)	4.92	0.44	263.30	11.27	<0.001	✓
	Location: Time (Park: Afternoon)	0.86	0.61	263.07	1.42	0.157	–
	Location: Time (Park: Evening)	1.21	0.62	263.10	1.96	0.051	–
Relative humidity (%)	Intercept	67.93	1.45	28.12	46.75	<0.001	✓
	Location (Park)	−0.53	1.41	263.15	−0.37	0.710	–
	Time (Afternoon)	−24.46	1.38	264.32	−17.68	<0.001	✓
	Time (Evening)	−15.84	1.39	264.35	−11.39	<0.001	✓
	Location: Time (Park: Afternoon)	3.08	1.93	263.06	1.59	0.12	–
	Location: Time (Park: Evening)	1.26	1.97	263.43	0.64	0.522	–
CO_2 (ppm)	Intercept	493.25	8.07	18.46	61.15	<0.001	✓
	Location (Park)	−22.15	6.03	263.15	−3.67	<0.001	✓
	Time (Afternoon)	−28.73	5.92	263.73	−4.86	<0.001	✓
	Time (Evening)	−34.76	5.95	263.74	−5.85	<0.001	✓
	Location: Time (Park: Afternoon)	0.86	8.27	263.10	0.10	0.917	–
	Location: Time (Park: Evening)	10.89	8.41	263.28	1.30	0.197	–
PM_1 (μg/m^3)	Intercept	4.04	0.57	11.79	7.09	<0.001	✓
	Location (Park)	−0.29	0.31	226.00	−0.94	0.347	–
	Time (Afternoon)	−1.06	0.30	226.89	−3.59	<0.001	✓
	Time (Evening)	−0.99	0.33	226.84	−3.05	<0.001	✓
	Location: Time (Park: Afternoon)	0.29	0.41	226.00	0.70	0.486	–
	Location: Time (Park: Evening)	−0.31	0.47	226.13	−0.65	0.515	–
$PM_{2.5}$ (μg/m^3)	Intercept	5.65	0.57	11.995	9.85	<0.001	✓
	Location (Park)	−0.57	0.31	226.02	−1.80	0.072	–
	Time (Afternoon)	−1.78	0.30	226.94	−5.85	<0.001	✓
	Time (Evening)	−1.66	0.33	226.89	−4.97	<0.001	✓
	Location: Time (Park: Afternoon)	0.56	0.42	226.02	1.33	0.184	–
	Location: Time (Park: Evening)	−0.05	0.48	226.15	−0.11	0.913	–
PM_{10} (μg/m^3)	Intercept	14.24	1.28	11.28	11.12	<0.001	✓
	Location (Park)	−0.81	0.63	226.02	−1.28	0.202	–
	Time (Afternoon)	−5.29	0.61	226.75	−8.68	<0.001	✓
	Time (Evening)	−4.92	0.67	226.71	−7.35	<0.001	✓
	Location: Time (Park: Afternoon)	0.27	0.85	226.02	0.32	0.749	–
	Location: Time (Park: Evening)	0.39	0.97	226.12	0.41	0.686	–

[a] Estimate = Model coefficient indicating effect size.
[b] df = Degrees of Freedom, representing the effective sample size used to estimate the parameter and test statistic in the mixed model.

3.3. Spatial gradients of heat and air pollution across park and built-up area

The spatial gradients of air temperature and relative humidity, CO_2 levels and PM concentrations, derived from spatial aggregation are shown in Fig. 5a–f. By utilising a 20-m hexagonal tessellation and a minimum data density filter (> 3 observations per cell), these maps represent the persistent environmental signatures of the study site. The figure highlights how the park environment contributes to reductions in air temperature, CO_2, and PM concentrations compared to the surrounding built-up areas. These spatial patterns reveal a clear decrease in these environmental parameters with increasing distance from the built-up area into the park, underscoring the crucial role of the park in mitigating heat and influencing local air quality.

The spatial distribution of air temperature, relative humidity, CO_2, PM_1, $PM_{2.5}$, and PM_{10} across the study area (Fig. 5a–f) reveals a distinct gradient associated with proximity to the park's centre. The PM concentrations and air temperatures were consistently lower toward the central zone of the park, reaching their minimum values along the middle axis. These relationships were observed over a distance of up to 240 m from the park's centre. Conversely, as the distance from the park increased - by transecting into the built-up area - these values showed a gradual rise, while relative humidity declined, with this pattern evident up to 300 m beyond the park edge. This pattern indicates clear spatial cooling and suggests localised improvements in air quality conditions. These results underscore the significance of analysing spatial variation in urban heating and air pollution levels with increasing distance from the park, highlighting the relevance of distance-based approaches as discussed in Section 3.4.

3.4. Distance-based analysis of air temperature and air pollution

Regression analyses were used to examine how various microclimate and air pollution parameters change with distance from the park during morning, afternoon, and evening periods (Fig. 6). Linear regression models were fitted to quantify trends, with slope estimates, confidence intervals, and significance levels summarised in Table S3.

In the built-up area, air temperature showed a statistically significant positive association with distance from the edge of the park during the morning (rate = 0.0053 °C/m, $p < 0.001$) and afternoon (rate = 0.0052 °C/m, $p < 0.001$), indicating increasing air temperature with distance, a trend observed up to 300 m from the park edge. Within the Park, significant temperature increases with distance from the centre to the edge of the park were limited to the morning (rate = 0.0215 °C/m, $p = 0.022$), while afternoon and evening trends were not statistically significant (Table S3).

Relative humidity decreased significantly with distance from edge of the park into the built-up area during the morning (rate = −0.0197%/m, $p < 0.001$) and afternoon (rate = −0.014%/m, $p < 0.001$), consistent with lower moisture availability in more exposed locations [67,68]. The absence of a significant trend in the evening may be attributed to the stabilisation of humidity levels due to reduced solar radiation [69,70]. Conversely, in the park, relative humidity increased significantly with distance from the centre of the park in the morning (rate = 0.015%/m, p

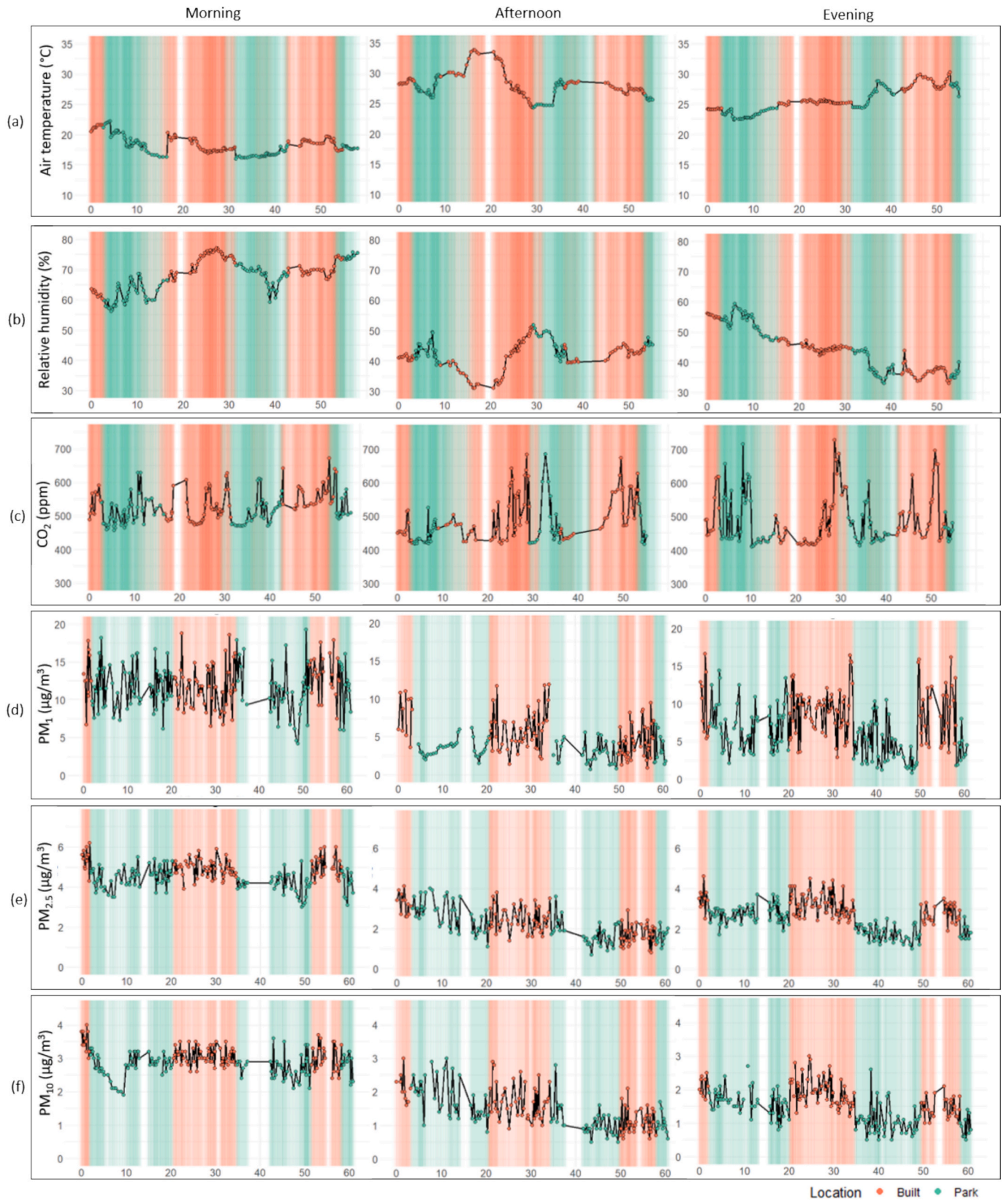

Fig. 4. Temporal variation of environmental parameters across three time periods (Morning, Afternoon, Evening) for two locations (Park and Built-up area) on a representative day (17th August for air temperature, relative humidity, and CO_2, and 25th August for PM levels). Each plot displays minute-by-minute values over a 60-min interval for (a) Air Temperature (°C), (b) Relative Humidity (%), (c) CO_2 (ppm), (d) PM_1 (µg/m^3), (e) $PM_{2.5}$ (µg/m^3), and (f) PM_{10} (µg/m^3). Data points are colour-coded by location, with shaded backgrounds indicating measurement zones (Park: green; Built-up area: orange).
(For interpretation of the references to colour in this figure legend, the reader is referred to the web version of this article.)

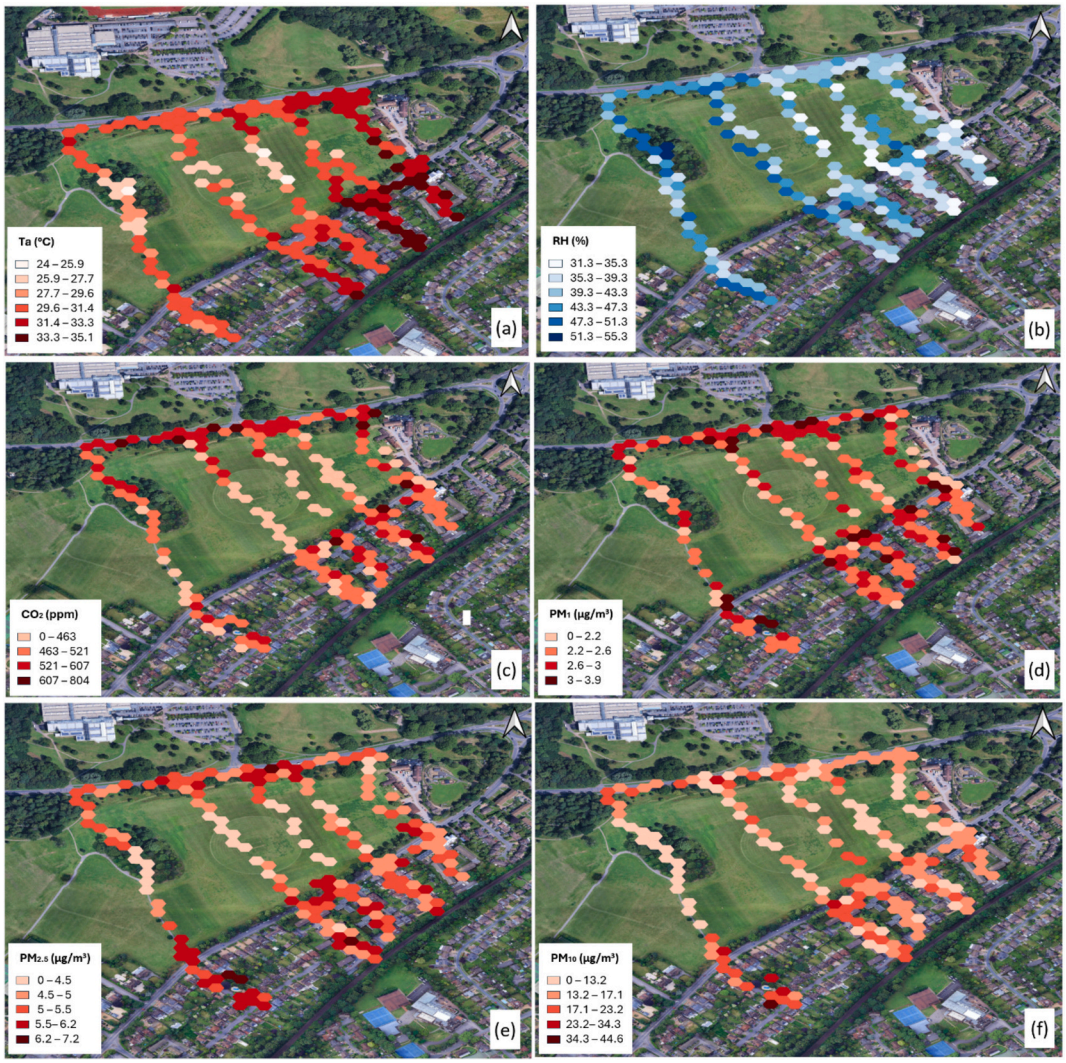

Fig. 5. The extent of park co-benefits in terms of heat mitigation and air pollution reduction. Maps represent the spatially aggregated mean values. Data are presented in a 20-m hexagonal tessellation for: (a) air temperature (°C), (b) relative humidity (%), (c) CO_2 (ppm), (d) PM_1 (µg/m^3), (e) $PM_{2.5}$ (µg/m^3), and (f) PM_{10} (µg/m^3). The maps illustrate spatial gradients in environmental conditions between the park and the surrounding built-up area.

< 0.001). No significant changes were detected in the afternoon or evening.

CO_2 concentrations in the built-up area decreased significantly with distance from the edge of the park (roadside) at all times of day (rates between −0.097 and − 0.169 ppm/m, $p < 0.001$). In contrast, the park exhibited significant positive trends for CO_2 at all times (slopes between 0.165 and 0.189 ppm/m, $p < 0.001$), likely reflecting enhanced biological respiration or localised CO_2 accumulation influenced by canopy structure [71,72].

PM showed more variable spatial patterns. PM_1 decreased significantly only during the evening by distance from the edge of the park into the built-up area (rate = −0.002 µg/m^3 per metre, $p = 0.009$). $PM_{2.5}$ showed a similar pattern with a significant evening decrease ($p = 0.04$), whereas no significant trends were observed during morning and afternoon periods. PM_{10} concentration decreased significantly with distance from the edge of the park (roadside) into the built-up area only in the evening (rate = −0.006 µg/m^3 per metre, $p = 0.008$), while trends in the park showed increasing pollutants level but there were not significant, likely due to the complex interplay of vegetation filtering, resuspension, and the proximity of the road near the park boundary acting as an intermittent emission source [73].

Overall, within the studied range up to 300 m from the park edge, a cooling effect of approximately 0.5 °C was estimated to occur within 100 m in the built-up area during morning hours, alongside a 1% increase in relative humidity within about 50 m. Evening PM concentrations decreased over 100 m, with PM_1, $PM_{2.5}$, and PM_{10} reduced by approximately 0.2 µg/m^3, 0.2 µg/m^3, and 0.6 µg/m^3, respectively. These results demonstrate clear spatial gradients in microclimate and air pollution parameters that vary by location and time of day, with the built-up area showing more pronounced increases in air temperature and decreases in relative humidity with distance from the park edge.

3.5. *Synergies and trade-offs among microclimatic and air quality services*

The exposure-adjusted analysis reveals pronounced spatial and temporal variation in how environmental services co-vary with distance from the park (Table S4). In the built-up area, strong and consistent synergies were identified between air temperature, relative humidity, and CO_2 across all times of day (EASI = +1.00). This indicates that distance-related cooling away from the park edge coincided with increased atmospheric moisture and reduced CO_2 concentrations, forming a bundle of microclimatic and gaseous benefits in the surrounding built-up area during morning and afternoon.

In contrast, PM levels exhibited systematic trade-offs with cooling benefit. In the morning, cooling showed strong opposition to PM_{10}

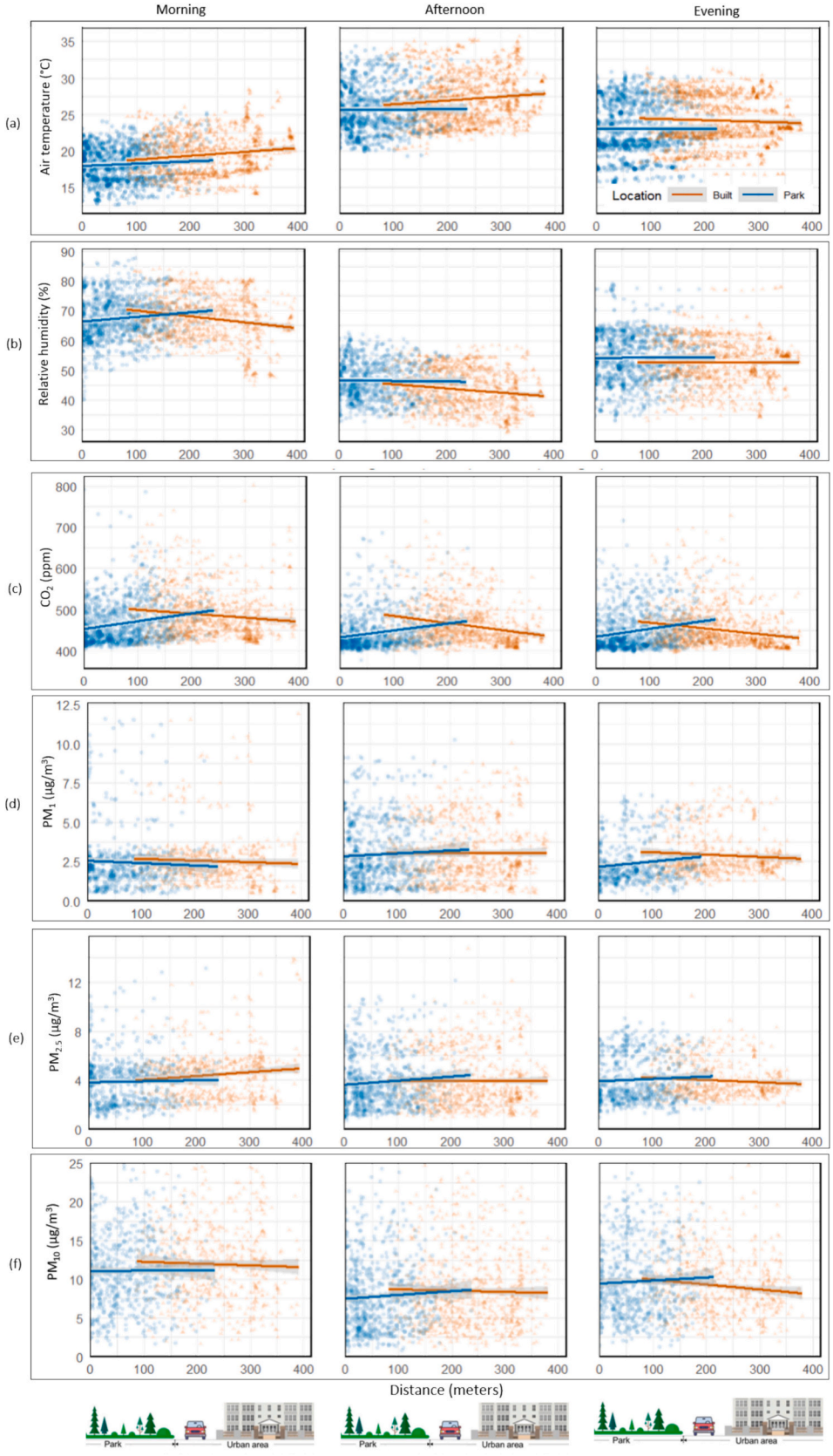

Fig. 6. Variation of (a) air temperature (°C), (b) relative humidity (%), (c) CO_2 concentration (ppm), (d) PM_1 (µg/m^3), (e) $PM_{2.5}$ (µg/m^3), and (f) PM_{10} (µg/m^3) with distance along measurement routes in built-up and park locations. Data points indicate individual measurements in Park (circles) and Built-up (triangles) locations. Lines represent moving averages, with shaded areas indicating 95% confidence intervals for linear trend lines across the morning, afternoon, and evening periods.

(EASI = −1.00) and moderate to strong trade-offs with $PM_{2.5}$ and PM_1, demonstrating that reductions in thermal exposure did not coincide with particulate matter mitigation. During the afternoon, PM levels weakened substantially (|EASI| < 0.4), indicating partial decoupling under peak thermal stress. In the evening, synergies re-emerged for PM_{10} (EASI = +1.00), while finer particles continued to display weaker or opposing responses, highlighting pollutant-size-dependent interactions.

Within the park interior, service interactions were more variable and strongly time dependent. Morning conditions exhibited moderate synergy between cooling and humidity (EASI = +0.36), while strong trade-offs were observed between cooling and both CO_2 and PM levels. During the afternoon, thermal–humidity synergy strengthened (EASI = +1.00), whereas trade-offs with all PM levels intensified, reflecting differing spatial gradients of cooling and PM levels within the park. Evening conditions showed a reconfiguration of interactions, with cooling aligning positively with CO_2 and PM_{10} but remaining opposed to $PM_{2.5}$, underscoring the temporal instability of multi-benefits coupling.

Overall, the results demonstrate that cooling represents the most spatially robust service, while air-quality benefits are edge-dominated, pollutant-specific, and temporally constrained. The quantified synergy and trade-off structure confirms that urban parks do not deliver uniform bundles of ecosystem services; instead, they generate context-dependent combinations whose effectiveness varies with location, time of day, and pollutant size.

3.6. Thermal comfort

The results based on the PET index revealed varied thermal perceptions across the different areas in the afternoon. In the built-up area, the thermal perception was categorised as 'warm' while the tree-shaded area fell into the 'comfortable' category, and the grassland was classified as 'slightly warm'. Comparing the PET values in these locations highlighted the effectiveness of the tree-shaded area and the grassland in reducing PET values by 8.5 °C and 4.5 °C, respectively, compared with the built-up area during the afternoon. This thermal variation is strongly linked to SVF values measured in each location: the tree-shaded area had a low SVF of 0.20, indicating dense canopy cover, while the grassland and built-up area had higher SVF values of 0.73 and 0.61, respectively. The relationship between SVF and temperature reduction is primarily influenced by radiative cooling, wind flow, and vegetation interactions [74,75].

Regression analyses revealed significant positive relationships between SVF and thermal comfort indices. For PET, slopes ranged from 4.06 to 10.6 across morning to afternoon ($p < 0.04$) indicating that a 0.1-

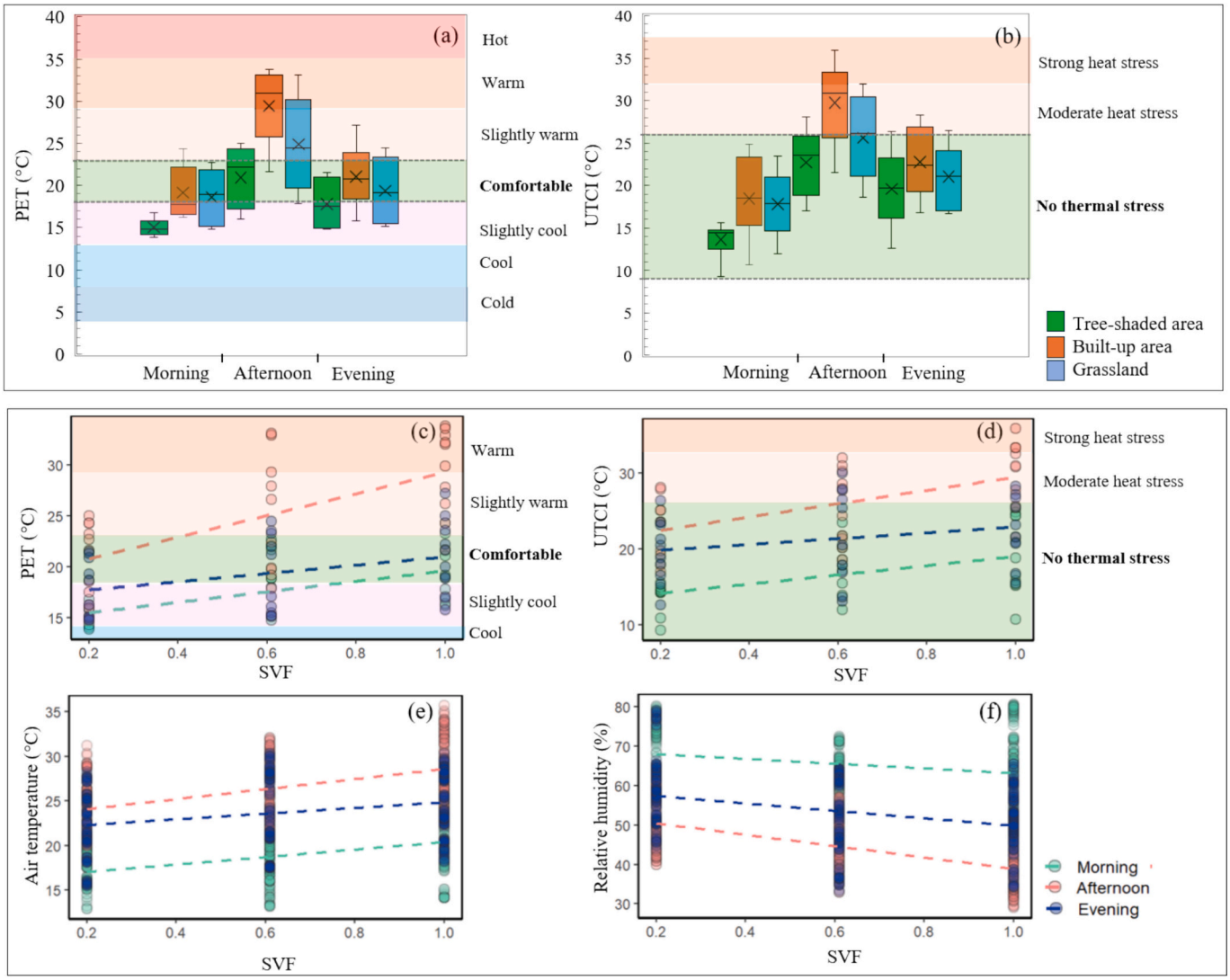

Fig. 7. (a) Boxplots of PET index and (b) UTCI index showing median (thick black line) and mean (cross), and scatter plots with linear regression lines of (c) PET against SVF, (d) UTCI against SVF, (e) air temperature against SVF, and (f) relative humidity against SVF. All measurements were taken during morning, afternoon, and evening at built-up areas, tree-shaded areas, and grassland locations.

unit increase in SVF corresponds to an increase in PET of approximately 0.41 to 1.06 °C, with the strongest effect in the afternoon. Similarly, the UTCI showed significant positive associations in the morning and afternoon (slopes 6.06 and 8.77, $p < 0.01$) with UTCI increasing by about 0.61 and 0.88 °C per 0.1-unit increase in SVF, respectively, while the evening relationship was not significant. Air temperature similarly exhibited a positive association with SVF throughout the day, with the strongest effect in the afternoon — a 0.1-unit increase in SVF corresponded to a 0.56 °C rise in temperature, indicating that greater sky exposure intensifies heat. Conversely, relative humidity was negatively associated with SVF, with a 0.1-unit increase linked to a 1.44% decrease during the afternoon (Fig. 7c–f). These results underscore the important role of urban geometry in shaping microclimatic and thermal comfort conditions, especially during peak thermal periods.

In the morning, PET values indicated that both the built environment and grassland were in the 'comfortable' category, while the tree-shaded area had a PET value of 4.09 °C lower than the built environment, falling into the 'slightly cool' category. By the evening, PET values for all three areas were nearly in the 'comfortable' category.

The results based on UTCI thermal stress categorisation across different areas reveal that all three areas -built environment, tree-shaded area, and grassland- fell within the 'no thermal stress' category during morning and evening. However, in the afternoon, the average UTCI in the built environment rose to the 'moderate heat stress' category, while the tree-shaded area and grassland remained in the 'no thermal stress' category. Comparing the efficacy of trees and grassland in improving thermal comfort conditions indicates that trees were more effective than grass. The average UTCI in the shade of trees was 4.2 °C lower compared to the grassland in the morning, 2.9 °C in the afternoon, and 1.5 °C in the evening. This indicates that tree-shaded areas consistently provide significantly better thermal comfort conditions throughout the day, which is in line with the finding that tree shade is necessary to reduce heat stress during the hot season, as solar radiation has a strong negative impact on thermal comfort [23,76].

Overall, PET and UTCI index values across all measurements collected during morning, afternoon, and evening show that trees and grassland have the most significant impact on improving thermal comfort conditions during the afternoon when air temperatures peak. Results indicate that PET and UTCI were reduced by up to 28.8% and 15.4%, respectively, in the tree-shaded area, and up to 23.6% and 13.8%, respectively, in the grassland compared to the built-up area.

Paired *t*-tests were conducted for both PET and UTCI indices across morning, afternoon, and evening periods to evaluate differences in thermal comfort conditions between the built-up area and park locations. Results revealed statistically significant reductions in thermal comfort conditions in the park locations during the afternoon and evening. In particular, both PET and UTCI values were significantly lower in the tree-shaded area and grassland compared to built-up areas during these times ($p < 0.01$), with the greatest differences observed in the afternoon (e.g., PET: mean difference = −8.18 °C, $p < 0.001$ for grassland vs built-up area). Morning differences were less consistent, with only UTCI in the grassland showing a statistically significant reduction compared to the built-up area (Table S5). These findings highlight the role of parks in improving thermal comfort conditions, especially during the afternoon.

However, as discussed in Section 3.1, humidity levels in the park were 3.2% higher in the afternoon. While the humidifying effects of vegetation can increase thermal discomfort, the reduction in air temperature due to evapotranspiration, combined with lower solar radiation exposure (reflected in reduced SVF), can offset this negative effect and lead to an overall improvement in thermal comfort [77].

3.7. Noise mitigation

Fig. 8a presents a comparison of mean noise levels across park and built-up areas during the morning, afternoon, and evening, with 95% confidence intervals as $L_{Aeq\text{-}30s}$. The built-up area consistently exhibited higher average noise levels than the park. The difference was most pronounced in the evening, where the built-up area recorded a mean of 69.5 dB (95% CI: 66.9–72.1), compared to 45.6 dB in the park (95% CI: 32.7–58.5). These observations align with previous studies showing that urban built-up areas typically experience higher noise levels compared to parks, especially during peak traffic hours [78,79]. During the morning, mean levels were 63.7 dB (95% CI: 62.9–64.4) in the built-up area and 59.4 dB (95% CI: 58.0–60.8) in the park. This pattern corresponds with findings that noise pollution peaks during morning and evening commutes, posing potential health risks [80]. Afternoon values were generally lower, with means of 62.0 dB (95% CI: 60.1–63.9) and 58.3 dB (95% CI: 57.5–59.1) in the built-up area and park, respectively. Statistical analysis confirmed these differences, with a Welch Two Sample *t*-test indicating that noise levels were significantly higher in the built-up area compared to the park ($t = 9.36$, df = 525.43, $p < 0.001$), with mean noise values of 63.7 dB and 58.6 dB, respectively.

In order to evaluate the noise levels by distance from the main road, Fig. 8b illustrates the distribution of noise levels by location and distance from the main road, overlaid with linear trendlines and 95% confidence intervals. Across all distances (<50 m, 50 to 100 m, and 100-200 m), noise levels were consistently lower in the park compared to the built-up

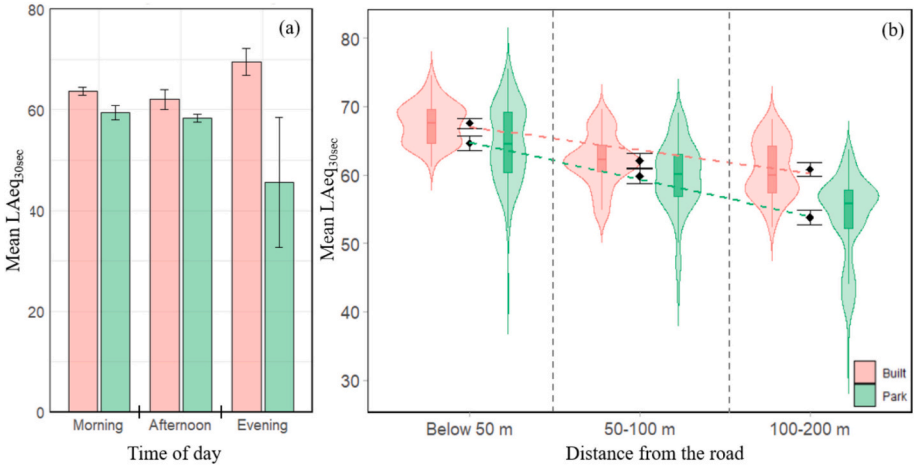

Fig. 8. (a) Bar plot showing mean $LAeq_{30sec}$ (dB) by time of day and location -error bars show 95% confidence intervals. (b) Violin plot illustrates the distribution and density of noise levels by distance and location. The violin plots are overlaid with boxplots to show median and interquartile ranges, and mean values are marked by points with 95% confidence intervals as error bars. Dashed trendlines represent linear trends in mean noise levels across distance from the road for each location.

area. The violin plots demonstrate that while both environments exhibit some variability, the central tendency in the park shifts more significantly downward with increasing distance from the road. This is also supported by the linear trend analysis. The fitted linear models indicate a steeper decline in noise levels with increasing distance from the road in the park (estimate = −5.41 dB/100 m, $p < 0.001$) compared to the built-up area (estimate = −3.40 dB/100 m, $p < 0.001$). Together, the temporal and spatial analyses underscore the crucial role of parks in mitigating road traffic noise.

Nevertheless, it should be noted that $LAeq_{30sec}$ represents overall sound exposure, integrating traffic and other environmental sources. Therefore, while the observed attenuation in the park is consistent with vegetation and terrain effects, some variability may also arise from fluctuations in traffic or non-traffic noise.

4. Discussion

4.1. Microclimate regulation

The observed morning and afternoon air temperature reduction of 1.3 °C within the park confirms the primary hypothesis that parks function as a thermal buffer against urban overheating. This thermodynamic divergence is driven by the interception of shortwave solar radiation by the vegetative canopy and the simultaneous partitioning of sensible heat into latent heat through amplified transpiration fluxes [81].

The high statistical significance of the location type within the LMM ($p < 0.001$) confirms that the park acts as the primary driver of this thermal discrepancy. This pattern is supported by the meta-analysis done by Bowler et al. [46] and the microclimatic evaluations done by Santamouris [82], which established that urban parks reduce ambient air temperatures by 0.5 °C to 1.5 °C in temperate climate zones. These localised temperature differences strongly underscore the real-world efficacy of parks in mitigating urban atmospheric overheating, an environmental regulation phenomenon widely conceptualised as the "park cool island" effect [83,84]. The 1.3 °C cooling magnitude recorded in this study aligns closely with the broader literature consensus, which establishes that urban parks can reduce ambient air temperatures by 0.6 °C to 7 °C compared to built-up area at various diurnal intervals depending on background macroclimatic baselines and local tree canopy structure [6,29,85–88]. Conversely, the non-significant effect of location on relative humidity ($p = 0.7$), contrasted with its high temporal significance ($p < 0.001$), supports the empirical assertions of Sahani et al. [89] that macroclimatic diurnal variations and regional air mass properties exert a stronger control over absolute atmospheric moisture capacity than localised vegetative inputs. However, the significant morning increase in relative humidity with distance from the centre of the park (0.015%/m, $p < 0.001$) captures a localised exception. The morning gradient is driven by the park's open centre, which allows rapid solar exposure and dew evaporation, whereas the denser, shaded park edges shelter the micro-environment and trap moisture under a stable morning boundary layer [46,90]. As solar irradiance intensifies in the afternoon, robust vertical convective mixing homogenises the water vapour across the park-urban interface, neutralising this spatial gradient [90].

The thermal comfort differences recorded between internal park locations—open grassland versus tree-shaded configurations—highlight the importance of landscape type. While open grasslands support rapid nocturnal radiative cooling due to their unobstructed exposure to the skyward dome, their elevated SVF permits substantial downwelling shortwave radiation during peak daylight hours.

In contrast, the tree-shaded area achieved a 2.9 °C lower afternoon UTCI compared to open grassland. This variance confirms the baseline thermal comfort hypothesis, demonstrating that blocking direct and scattered shortwave radiation via canopy structures provides superior pedestrian relief than an unshaded grass lawn. This outcome aligns with the findings of Morakinyo et al. [91] and Abdallah et al. [92], which demonstrated that optimising tree canopy density and minimising the SVF are the primary design interventions for lowering outdoor heat stress. This relationship is further supported by the strong positive correlation established between SVF and the outdoor thermal stress metrics ($r > 0.78$, $p < 0.01$), confirming that urban canopy openness drives microscale pedestrian heat strain under high solar loads [93]. SVF's role in urban climate adaptation using trees is a key strategy to mitigate urban heat, as the higher canopy density associated with lower SVF promotes air temperature reduction through enhanced ventilation and radiative cooling [94].

4.2. Temperature and air pollution spatial gradient

The spatial gradient analysis indicates clear spatial cooling and suggests localised improvements in air quality conditions. These variations are strongly influenced by local land cover characteristics and the surrounding urban configuration. Previous studies have shown that air temperature is closely linked to surface characteristics, with increased vegetation cover leading to lower temperatures and higher proportions of impervious surfaces correlating with elevated temperatures [88]. The structure and land use of the surrounding urban environment significantly shape both the cooling intensity and spatial extent of a park's influence [88,95]). Anthropogenic heat sources and dense urban morphology can further constrain airflow and limit the distribution of cool air into adjacent areas [86,96]. Materials such as concrete and asphalt, common in built-up areas, can further amplify thermal exposure by storing and re-emitting heat throughout the day [97].

Furthermore, wind speed and direction, as well as the traffic exposure of the roads, play a critical role in modulating pollutants' spatial patterns. Norouzi et al. [98] highlighted the importance of considering wind as a site-related factor that can enhance or suppress the performance of urban parks. In this context, the observed spatial gradients reflect not only the park's inherent ecological functions but also its dynamic interactions with surrounding green infrastructure and urban settings [95,99,100].

The distance-based analysis shows a significant temperature increase exceeding 0.5 °C per 100 m (0.005 °C/m) as measurements move away from the park edge into the built-up area during morning and afternoon. These findings align with previous studies reporting a cooling effect of urban parks, where ambient air temperature gradually increases with distance from the park border, highlighting the park's moderating influence on adjacent urban environments [88,101].

The distance-based analysis indicates that the park's cooling influence extends up to 300 m into the surrounding built-up area. This spatial extension supports the empirical models of Doick et al. [102] for London parks and Qiu et al. [47] for East Asian urban settings, which concluded that the thermal mitigation footprint of a macroscale park regularly projects between 200 and 400 m into adjacent high-density built environmnet. Furthermore, this dynamic matches the trends observed by Pfautsch et al. [27] in temperate and semi-arid urban interfaces, where sharp horizontal microclimatic gradients settle within a 300-m threshold before encountering complete absorption by surrounding low-albedo building envelopes. The evening period showed a non-significant slight decrease in temperature, which may result from nocturnal cooling effects and stable atmospheric conditions diminishing spatial gradients [70].

Collectively, the magnitude and rate of changes in distance-based analysis for all the recorded parameters are influenced by a complex interplay of factors including climate conditions, park characteristics, land cover composition, adjacent urban structures, prevailing wind patterns, traffic emissions, and canopy density [103–105], underscoring the need for context-sensitive assessments when evaluating how urban parks mitigate environmental stressors. While these findings suggest that parks can provide improvements in microclimate regulation and local air pollution exposure, the extent to which park geometry and

placement influence the reach of these benefits beyond 300 m from park boundaries remains a subject for further investigation to optimise user exposure to such mitigation gradients.

4.3. Air pollution dynamics

Air pollutants showed different spatial behaviours across the park boundary, indicating distinct dispersion mechanisms for gases and particulate matter. The significant reduction of gaseous CO_2 inside the park (2.3% to 3.3%, $p < 0.001$) reflects variations in anthropogenic activity and carbon uptake by plants [106,107]. CO_2 reductions observed in the park during the evening, when photosynthetic activity is minimal, are attributed to lower local emissions and increased atmospheric dispersion within vegetated areas. This pattern aligns with the spatial observations reported by Sahani et al. [89], which showed that central park zones consistently experience lower concentrations of traffic related pollutants due to their increased distance from adjacent road networks.

Conversely, the lack of a statistically significant main location effect for PM_{10}, $PM_{2.5}$, and PM_1 within the LMM indicates that daytime particulate concentrations are primarily governed by regional background levels and mesoscale atmospheric mixing. This pattern is supported by the findings of Xing and Brimblecombe [19], who noted that daytime boundary layer instability and convective mixing often override the localised filtration benefits of urban vegetation. This lack of a uniform daytime location effect is tied to pronounced diurnal fluctuations in boundary layer dynamics influenced by environmental context and traffic emission intensity [108]. Additionally, anthropogenic influences, particularly traffic-related emissions from the road separating the park and built-up area, not only contribute to the complexity of PM dispersion but also constitute a major source of PM [109]. The higher particulate reductions observed during the morning intervals are likely driven by the concentrated surge of mobile combustion emissions near peripheral road networks during early periods of lower atmospheric dispersion; because the park core is physically set back from these primary sources, it remains relatively cleaner, yielding a sharp horizontal gradient across the boundary. As the day progresses, higher wind speeds and stronger convective mixing likely promote vertical and horizontal dispersion, thereby reducing near-surface PM gradients [110,111]. Occasional peaks within the park for PM_1 indicate localised resuspension or micro-scale variability. Collectively, while these patterns suggest a potential role for urban vegetation in particulate sequestration, the lack of statistical significance highlights that these effects are secondary to the complex interactions between local emission sources, pollutant dynamics, and the modulating effects of wind and mixing conditions [110,112,113].

However, the emergence of a significant distance-dependent PM gradient during evening hours ($p < 0.05$) reveals a clear temporal shift in transport dynamics. As the ground cools and the atmospheric boundary layer stabilises, convective mixing decreases, allowing the dense vegetation of the park to serve as an effective dry deposition filter and a physical barrier to dispersion. This stable nocturnal condition restricts the penetration of fine particulates (PM_1) into the park core at a predictable spatial rate of -0.002 μg/m^3 per metre, creating a protected microscale zone for pedestrians. This dual-regime interaction aligns with both the macroscale boundary layer observations of Janhäll [114] and the near-road microscale barrier models of Abhijith et al. [115].

4.4. Noise attenuation

The substantial acoustic buffering effect observed within the park, where evening sound pressure levels were 23.9 dB lower than those recorded within the adjacent built-up area, reflects the combined influence of surface characteristics and differences in anthropogenic activity between the two environments. The hard, non-porous surfaces of the built-up area retain and reflect sound energy [116]. In contrast, the park environment exhibited an attenuation rate of −5.41 dB per 100 m ($p < 0.001$).

The greater slope in the park reflects stronger attenuation, likely due to the presence of vegetation, uneven terrain, and softer ground surfaces, which enhance acoustic absorption and diffusion—contrasting with the reflective surfaces common in built-up areas [117–119]. In the built-up area, the observed gradient is driven primarily by increasing distance from the main road—a dominant source of traffic noise—as well as by variations in building density, street geometry, and surface materials, which influence sound attenuation [120,121]. The observed attenuation gradient is consistent with the findings of Cohen et al. [34] and Margaritis and Kang [122], who reported sound pressure level reductions ranging from 4.0 to 6.0 dB per 100 m within vegetated urban environments. The results also support the acoustic shielding framework proposed by Van Renterghem et al. [123], which demonstrated that soft ground surfaces contribute substantially to low-frequency noise attenuation through ground impedance transitions, while tree belts enhance the scattering of higher-frequency traffic noise.

The temporal variability of these multi-benefits was further reflected in the EASI. The persistent morning trade-off (EASI = −1.00) near the park perimeter suggests that cooling benefits may coincide with elevated pollutant exposure along major traffic corridors bordering the park. The decoupling of these parameters during the afternoon, followed by the re-emergence of synergistic conditions in the evening (EASI = +1.00), demonstrates that multi-benefit provision is highly dynamic and governed by diurnal changes in atmospheric stability and localised emission patterns. These findings reinforce the multi-benefit optimisation frameworks proposed by Demuzere et al. [124] and Kumar et al. [125].

4.5. Limitations and future research

This study contributes to advancing the understanding of environmental gradients across the park–urban interface by integrating high-resolution, pedestrian-level mobile monitoring with a multi-parameter exposure framework. In contrast to conventional approaches based on stationary monitoring stations or remotely sensed data, this framework enables the simultaneous quantification of microclimatic conditions, air quality, and acoustic variability along continuous spatial transects, thereby capturing environmental exposure as experienced in situ [126]. This methodological advancement supports a more process based and human-centred characterisation of urban ecosystem services and strengthens the empirical basis for evaluating park performance in complex urban settings.

Despite these contributions, several limitations should be considered when interpreting the results. The transect-based mobile monitoring approach successfully resolved fine-scale spatial heterogeneity; however, measurements were confined to a single seasonal window. Data collection was conducted during the summer period (August–September), capturing conditions associated with peak thermal stress but not representing winter microclimates or interseasonal variability in park function. Seasonal dynamics in vegetation structure, particularly changes in leaf area index and deciduous phenology, are expected to substantially influence shading, evapotranspiration, pollutant deposition, and acoustic attenuation [127]. Moreover, Measurements were conducted during the summer school vacation period to capture high-temperature conditions, which may also coincide with reduced traffic-related emissions; greater contrasts in pollutant concentrations may therefore be expected during non-vacation periods. As a result, the observed gradients should be interpreted as season-specific rather than universally representative. Future studies incorporating multi-seasonal and multi-annual monitoring would be essential to establish the temporal robustness and climatic sensitivity of the identified patterns.

Temporal coverage also represents a defined analytical scope. The monitoring design focused on morning, afternoon, and evening periods, providing a robust representation of daytime diurnal variability, but

excluding nocturnal and early dawn conditions. These periods are characterised by stable boundary layer development and atmospheric inversions, which can influence pollutant accumulation, surface energy exchange, and near-surface turbulence structure [128]. Inclusion of these transition periods in future studies would further refine the understanding of full diurnal system dynamics.

From an analytical perspective, the use of first-order polynomial and linear regression modelling provided a transparent and physically interpretable basis for identifying dominant spatial gradients. While effective for characterising monotonic trends, some relationships likely reflect more complex, non-linear interactions at the vegetated–built interface. Such behavior is expected given the coupled nature of radiative forcing, turbulence structure, and vegetation heterogeneity [129]. Future research incorporating non-linear modelling approaches and larger multi-site datasets would enable more detailed resolution of threshold effects and interaction driven dynamics.

In addition, the absence of vertical profiling limits the interpretation of how near-surface exposure gradients interact with canopy layer and boundary layer processes. Coupling mobile ground measurements with LiDAR-derived structural data and unmanned aerial vehicle-based observations would enable fully three-dimensional characterisation of urban environmental regulation and improve mechanistic understanding of vegetation mediated modifications.

Finally, the results highlight important opportunities for aligning ecosystem service provision with human activity patterns. The observed temporal structuring of benefits, with stronger thermal comfort in the late afternoon and more consistent air quality improvements in the morning, suggests that different environmental functions peak at different times of day. This temporal differentiation has direct implications for urban design and park management strategies. Future research integrating environmental exposure data with behavioural observations and health relevant indicators, including mobility patterns and physiological responses, would enable a more comprehensive understanding of how spatial environmental gradients translate into lived experience and public health outcomes.

5. Summary and conclusions

This research employed mobile environmental monitoring techniques to quantify the capacity of public urban green spaces to reduce summer heat and thereby improve human thermal comfort, influence local air quality conditions, and mitigate noise pollution. These benefits were calculated using distance-based analyses and contrasting measurements from green space with those collected in nearby built environments. While similar findings to this work, including the significant effect of the park to cool the air, reduce urban heat island effects or reduce ambient noise, have been reported in other studies, the unique and highly valuable contribution of this work is in quantifying these benefits per unit of distance at high granularity. Estimating the magnitude of the benefits for distances that become relevant to landscape architects, city planners, and public health professionals means that data presented here can now inform heat-, noise- and pollution-responsive urban landscape design. Such an evidence-based approach to the design and construction of urban parks and adjacent residential zones leads to greater community benefits and thus improved resilience.

Linear Mixed Models indicated that air temperature was consistently lower in the park than in the built-up area (−1.89 °C). Time of day strongly affected temperature, relative humidity, and CO_2, with afternoon values reflecting peak thermal stress, while interaction effects were generally non-significant for temperature and humidity, indicating consistent diurnal patterns across locations. In contrast, location effects on PM concentrations were not statistically significant, suggesting that particulate matter mitigation by the park was not uniform across all conditions. The observed distance-based gradients indicate that maximising the park interior relative to its boundary can help maintain the temperature and noise reductions identified in this study. In constrained urban spaces, these results suggest that walking routes in parks can be designed with increased length or looped configurations. Such layouts can maximise the time a user spends within beneficial microclimates—such as tree-shaded zones—without requiring an increase in the total land area of the park.

Based on distance-based analysis, knowing that air temperature will rise 0.5 °C for every 100 m of distance from the park can be used to support stronger regulations and incentives to include more green infrastructure in the built environment. The analysis also revealed localised evening reductions in PM levels (up to 0.6 $\mu g/m^3$). While overall location effects on PM concentrations did not reach statistical significance, distance-based analyses revealed persistent spatial gradients across different periods, most notably in the evening. These patterns suggest that the park's influence on air quality is characterised by spatial heterogeneity rather than a uniform reduction. Such gradients imply that the level of pollution exposure for park users is highly dependent on their proximity to the park core, where more distinct signatures of PM mitigation provide localised micro-environments of reduced PM exposure. Additionally, the park reduced noise levels by more than 3 dB per 100 m away from roads, which is physically significant as a 3 dB decrease corresponds to a halving (factor of 2) of sound intensity, although it represents a smaller change in sound pressure level and the perceived loudness for the human ear. These findings can inform the layout of roads, street blocks and green spaces in new suburbs. Furthermore, analysis of cooling–air pollution relationships demonstrated that cooling benefits did not consistently coincide with PM reductions, highlighting context-dependent synergies and trade-offs between environmental services that vary with distance, time of day, and pollutant type.

In a warming world, and in addition to their value for recreation, public parks can now be designed as retreats from increasing noise pollution and heat stress. Recognising that environmental benefits are not uniformly co-delivered but instead exhibit spatially and temporally variable interactions is essential for effective planning. Specifically, park tracks and internal pathways can be strategically routed through cooling corridors, such as tree-shaded areas that this study found to reduce PET by up to 28.8%, ensuring that the primary transit routes used by pedestrians provide maximum thermal relief. Furthermore, aligning these tracks away from park edges can further leverage the observed 0.5 °C temperature increase and 3.4 dB noise decline found for every 100 m of distance from the built-up boundary. Including these functions deliberately in tender and design processes is a logical response to contemporary climate change and associated rising summer air temperatures. Future research should assist in further optimising the effectiveness of public parks in delivering the aforementioned benefits. This work should include investigating the interplay between park size and shape, vegetation composition and site management on air temperature, PM concentration and thermal comfort under local summer weather conditions. As demonstrated here, mobile monitoring equipment that records environmental data at high frequency will be an important tool in these investigations to capture short-term fluctuations and fine-scale spatial variability in microclimatic and air quality parameters, enabling reliable smoothing and interpretation of environmental gradients, supporting evidence-based planning and design of resilient urban landscapes.

CRediT authorship contribution statement

Soheila Khalili: Writing – review & editing, Writing – original draft, Visualization, Validation, Methodology, Formal analysis, Data curation, Conceptualization. **Laurence Jones:** Writing – review & editing, Supervision, Methodology, Investigation. **Sebastian Pfautsch:** Writing – review & editing, Methodology, Investigation, Conceptualization. **Prashant Kumar:** Writing – review & editing, Supervision, Project administration, Methodology, Investigation, Funding acquisition, Conceptualization.

Declaration of competing interest

The authors declare that they have no known competing financial interests or personal relationships that could have appeared to influence the work reported in this paper.

Acknowledgements

The authors acknowledge the support received from the SCENARIO DTP funding and the team from the University of Surrey's Global Centre for Clean Air Research (GCARE) to undertake Soheila Khalili's PhD programme. PK and LJ acknowledge the support received through the UKRI (NERC, EPSRC, AHRC) funded RECLAIM Network Plus (EP/W034034/1; EP/W033984/1), GreenCities (NE/X002799/1; NE/X002772/1), GP4Streets (UKRI1281) and GREENIN Micro Network Plus (UKRI1239) and UGPN-funded (GREENICON and UGPN-NBS) projects.

Appendix A. Supplementary data

Supplementary data to this article can be found online at https://doi.org/10.1016/j.cacint.2026.100407.

Data availability

Data will be made available on request.

References

[1] World Health Organization. (2025). Urban planning. WHO. Retrieved February 3, 2025, available online at: https://www.who.int/teams/environment-climate-change-and-health/healthy-urban-environments/urban-planning.
[2] Klemm W, Lenzholzer S, van den Brink A. Developing green infrastructure design guidelines for urban climate adaptation. J Landsc Archit 2017;12:60–71.
[3] Oijstaeijen W, Van Passel S, Cools J. Urban green infrastructure: a review on valuation toolkits from an urban planning perspective. J Environ Manag 2020;267:110603.
[4] Bowler DE, Callaghan CT, Felappi JF, Mason BM, Hutchinson R, Kumar P, et al. Evidence-base for urban green-blue infrastructure to support insect diversity. Urban Ecosyst 2024;28:1–14.
[5] Hansen R, Pauleit S. From multifunctionality to multiple ecosystem services? A conceptual framework for multifunctionality in green infrastructure planning for urban areas. Ambio 2014;43:516–29.
[6] Kumar P, Corada K, Debele S, Emygdio APM, Abhijith KV, Broomandi P, et al. Air pollution abatement from green-blue-grey infrastructure. Innov Geosci 2024;2(4):100100.
[7] Aghamohammadi N, Santamouris M, editors. Mitigation and adaptation of urban overheating - the impact of warmer cities on climate, energy, health, environmental quality, economy, and quality of life. Amsterdam: Elsevier; 2024. p. 380.
[8] Sahani J, Kumar P, Debele SE. Efficacy assessment of green-blue nature-based solutions against environmental heat mitigation. Environ Int 2023;179:108187.
[9] Zölch T, Maderspacher J, Wamsler C, Pauleit S. Using green infrastructure for urban climate-proofing: an evaluation of heat mitigation measures at the micro-scale. Urban For Urban Green 2016;20:305–16.
[10] Shi M, Chen M, Jia W, Du C, Wang Y. Cooling effect and cooling accessibility of urban parks during hot summers in China's largest sustainability experiment. Sustain Cities Soc 2023;93:104519.
[11] Shi M, Wang Y, Lv H, Jia W. Climate gentrification along with parks' cooling performance in one of China's tropical industrial cities. Sci Total Environ 2023;892:164603.
[12] Manoli G, Fatichi S, Schläpfer M, Yu K, Crowther TW, Meili N, et al. Magnitude of urban heat islands largely explained by climate and population. Nature 2019;573(7772):55–60.
[13] Jones L, Anderson S, Læssøe J, Banzhaf E, Jensen A, Bird DN, et al. A typology for urban green infrastructure to guide multifunctional planning of nature-based solutions. Nat Based Solut 2022;2:100041.
[14] Chen M, Jia W, Yan L, Du C, Wang K. Quantification and mapping cooling effect and its accessibility of urban parks in an extreme heat event in a megacity. J Clean Prod 2022;334:130252.
[15] Gao Z, Zaitchik BF, Hou Y, Chen W. Toward park design optimization to mitigate the urban heat Island: Assessment of the cooling effect in five US cities. Sustain Cities Soc 2022;81:103870.
[16] Li Y, Fan S, Li K, Zhang Y, Kong L, Xie Y, et al. Large urban parks summertime cool and wet island intensity and its influencing factors in Beijing, China. Urban For Urban Green 2021;65:127375.
[17] Sugawara H, Narita KI, Mikami T. Vertical structure of the cool island in a large urban park. Urban Clim 2021;35:100744.
[18] Pierce AM, Loría-Salazar SM, Holmes HA, Gustin MS. Investigating horizontal and vertical pollution gradients in the atmosphere associated with an urban location in complex terrain, Reno, Nevada, USA. Atmos Environ 2019;196:103–17.
[19] Xing Y, Brimblecombe P. Dispersion of traffic derived air pollutants into urban parks. Sci Total Environ 2018;622:576–83.
[20] Aram F, Solgi E, Baghaee S, García EH, Mosavi A, Band SS. How parks provide thermal comfort perception in the metropolitan cores: a case study in Madrid Mediterranean climatic zone. Clim Risk Manag 2020;30:100245.
[21] Aram F, Solgi E, Garcia EH, Mosavi A. Urban heat resilience at the time of global warming: evaluating the impact of the urban parks on outdoor thermal comfort. Environ Sci Eur 2020;32:1–15.
[22] Aram F, Solgi E, Higueras García E, Mosavi A, Várkonyi-Kóczy R, A.. The cooling effect of large-scale urban parks on surrounding area thermal comfort. Energies 2019;12:3904.
[23] Chan SY, Chau CK, Leung TM. On the study of thermal comfort and perceptions of environmental features in urban parks: a structural equation modeling approach. Build Environ 2017;122:171–83.
[24] Kumar N, James A, Nath S. Study on noise pollution level in parks of Allahabad city, India. Int Res J Environ Sci 2013;2:88–90.
[25] Margaritis E, Kang J, Filipan K, Botteldooren D. The influence of vegetation and surrounding traffic noise parameters on the sound environment of urban parks. Appl Geogr 2018;94:199–212.
[26] Tashakkor S, Chamani A, Nadoushan MA, Moshtaghie M. Acoustics in urban parks: Does the structure of narrow urban parks matter in designing a calmer urban landscape? Front Earth Sci 2020;14:512–21.
[27] Pfautsch, S., Wujeska-Klause, A., Walters, J. R. (2024). Mapping summer microclimates across the City of Sydney. Western Sydney University and City of Sydney. Retrieved May 25, 2026, available online at: https://www.cityofsydney.nsw.gov.au/research-reports/mapping-summer-microclimates.
[28] Wu Q, Huang Y, Irga P, Kumar P, Li W, Wei W, et al. Synergistic control of urban heat island and urban pollution island effects using green infrastructure. J Environ Manag 2024;370:122985.
[29] Kumar P, Debele S, Khalili S, Halios CH, Sahani J, Aghamohammadi N, et al. Urban heat mitigation by green and blue infrastructure: a review of drivers, effectiveness, and future needs. Int J Hydrogen Energ 2024;5(2):100588.
[30] Zhang J, Gou Z, Cheng B, Khoshbakht M. A study of physical factors influencing park cooling intensities and their effects in different time of the day. J Therm Biol 2022;109:103336.
[31] Guo A, Yue W, Yang J, Li M, Zhang Z, Xie P, et al. Quantifying the cooling effect and benefits of urban parks: a case study of Hangzhou, China. Sustain Cities Soc 2024;113:105706.
[32] Aram F, Solgi E, Baghaee S, García EH, Mosavi A. Band S.S. How parks provide thermal comfort perception in the metropolitan cores: a case study in Madrid Mediterranean climatic zone. Clim Risk Manag 2020;30:100245.
[33] Yin S, Shen Z, Zhou P, Zou X, Che S, Wang W. Quantifying air pollution attenuation within urban parks: an experimental approach in Shanghai, China. Environ Pollut 2011;159:2155–63.
[34] Cohen P, Potchter O, Schnell I. The impact of an urban park on air pollution and noise levels in the Mediterranean city of Tel-Aviv, Israel. Environ Pollut 2014;195:73–83.
[35] Zalakeviciute R, Bedoya SB, Coronel DM, Bastidas M, Buenano A, Diaz-Marquez A. Central parks as air quality oases in the tropical Andean city of Quito. Atmos Environ 2024;21:100239.
[36] Arsalan M, Chamani A, Zamani-Ahmadmahmoodi R. Sustaining tranquility in small urban green parks: A modeling approach to identify noise pollution contributors. Sustain Cities Soc 2024;113:105655.
[37] Wei H, Huang X, Wang S, Lu J, Li Z, Zhu L. A data-driven investigation on park visitation and income mixing of visitors in New York City. Environ Plan B Urban Anal City Sci 2022;50:796–813.
[38] Wilson J, Xiao X. The economic value of health benefits associated with urban park investment. Int J Environ Res Public Health 2023;20:4815.
[39] Guan C, Song J, Keith M, Akiyama Y, Shibasaki R, Sato T. Delineating urban park catchment areas using mobile phone data: a case study of Tokyo. Comput Environ Urban Syst 2020;81:101474.
[40] Zhu J, Lu H, Zheng T, Rong Y, Wang C, Zhang W, et al. Vitality of urban parks and its influencing factors from the perspective of recreational service supply, demand, and spatial links. Int J Environ Res Public Health 2020;17(5):1615.
[41] Earth Köppen. Köppen climate classification map. Retrieved May 21, 2025, available online at: https://koppen.earth/; 2025.
[42] Office for National Statistics (ONS). Guildford (E07000209): Local indicators. Retrieved June 8, 2026, available online at: https://www.ons.gov.uk/explore-local-statistics/areas/E07000209-guildford/indicators; 2026.
[43] Data Climate. Guildford climate (United Kingdom): data and graphs for weather & climate in Guildford. Retrieved December 16, 2025, available online at: https://en.climate-data.org/europe/united-kingdom/england/guildford-60140/; 2025.
[44] WeatherSpark Historical weather in August 2024 at London Heathrow Airport, United Kingdom. Retrieved June 8, 2026, available online at: https://weatherspark.com/h/m/147876/2024/8/Historical-Weather-in-August-2024-at-London-Heathrow-Airport-United-Kingdom; 2024.
[45] WeatherSpark. Historical weather summer 2023 at London Heathrow Airport, United Kingdom. Retrieved February 2, 2025, available online at: https://weatherspark.com/h/s/147876/2023/1/Historical-Weather-Summer-2023-at-London-Heathrow-Airport-United-Kingdom#Figures-WindDirection; 2023.

[46] Bowler DE, Buyung-Ali L, Knight TM, Pullin AS. Urban greening to cool towns and cities: a systematic review of the empirical evidence. Landsc Urban Plan 2010;97:147–55.
[47] Qiu X, Kil SH, Jo HK, Park C, Song W, Choi YE. Cooling effect of urban blue and green spaces: a case study of Changsha, China. Int J Environ Res Public Health 2023;20:2613.
[48] Verma R, Zawadzka JE, Garg PK, Corstanje R. The relationship between spatial configuration of urban parks and neighbourhood cooling in a humid subtropical city. Landsc Ecol 2024;39:34.
[49] Kim J, Lee DK, Brown RD, Kim S, Kim JH, Sung S. The effect of extremely low sky view factor on land surface temperatures in urban residential areas. Sustain Cities Soc 2022;80:103799.
[50] Oke TR. Street design and urban canopy layer climate. Energy Build 1988;11 (1–3):103–13.
[51] Khalili S, Fayaz R, Zolfaghari SA. Analyzing outdoor thermal comfort conditions in a university campus in hot-arid climate: a case study in Birjand, Iran. Urban Clim 2022;43:101128.
[52] Lam CKC, Lau KKL. Effect of long-term acclimatization on summer thermal comfort in outdoor spaces: a comparative study between Melbourne and Hong Kong. Int J Biometeorol 2018;62:1311–24.
[53] Ng E, Cheng V. Urban human thermal comfort in hot and humid Hong Kong. Energ Buildings 2012;55:51–65.
[54] Abhijith KV, Rawat N, Emygdio APM, Le Den C, Collins K, Cartwright P, et al. Demonstrating multi-benefits of green infrastructure to schools through collaborative approach. Sci Total Environ 2025;958:177959.
[55] Diong HT, Neitzel R, Martin WH. Spatial evaluation of environmental noise with the use of participatory sensing system in Singapore. Noise Mapp 2021;8:236–48.
[56] Du M, Hong B, Gu C, Li Y, Wang Y. Multiple effects of visual-acoustic-thermal perceptions on the overall comfort of elderly adults in residential outdoor environments. Energ Buildings 2023;283:112813.
[57] Zhang Y, Zhao H, Li Y, Long Y, Liang W. Predicting highly dynamic traffic noise using rotating mobile monitoring and machine learning method. Environ Res 2023;229:115896.
[58] WeatherSpark Average weather in Guildford, United Kingdom, year round. Retrieved June 7, 2026, available online at: https://weatherspark.com/y/45132/Average-Weather-in-Guildford-United-Kingdom-Year-Round; 2026.
[59] Bendl J, Neukirchen C, Mudan A, Padoan S, Zimmermann R, Adam T. Personal measurements and sampling of particulate matter in a subway–Identification of hot-spots, spatio-temporal variability and sources of pollutants. Atmos Environ 2023;308:119883.
[60] Liu X, Zhang X, Wang R, Liu Y, Hadiatullah H, Xu Y, et al. High-precision microscale particulate matter prediction in diverse environments using a long short-term memory neural network and street view imagery. Environ Sci Technol 2024;58:3869–82.
[61] Bröde P, Fiala D, Błażejczyk K, Kampmann B. Deriving the operational procedure for the Universal Thermal Climate Index (UTCI). Int J Biometeorol 2013;57: 407–14.
[62] Jing W, Qin Z, Mu T, Ge Z, Dong Y. Evaluating thermal comfort indices for outdoor spaces on a university campus. Sci Rep 2024;14:21253.
[63] Tousi E, Mela A, Tseliou A. Thermal stress in outdoor spaces during Mediterranean heatwaves: A PET and UTCI analysis of different demographics. Urban Sci 2024;8:193.
[64] Höppe P. The physiological equivalent temperature–a universal index for the biometeorological assessment of the thermal environment. Int J Biometeorol 1999;43(2):71–5.
[65] Nikolopoulou M. Outdoor thermal comfort. Front Biosci 2011;3:1552–68.
[66] ASHRAE. ANSI/ASHRAE standard 55: thermal environmental conditions for human occupancy. American Society of Heating, Refrigerating and Air-Conditioning Engineers; 2017.
[67] Melaas EK, Wang J, Miller DL, Friedl MA. Interactions between urban vegetation and surface urban heat islands: a case study in the Boston metropolitan region. Environ Res Lett 2016;11(5):054020.
[68] Wahyudi H, Jumadi J. Spatio temporal analysis of urban heat island using landsat 8 oli/tirs imagery in klaten district in 2013 – 2021. Int J Disaster Dev Interface 2024;4(1):1–12.
[69] Alavipanah S, Wegmann M, Qureshi S, Weng Q, Koellner T. The role of vegetation in mitigating urban land surface temperatures: a case study of Munich, Germany during the warm season. Sustainability 2015;7:4689–706.
[70] Sun T, Sun R, Chen L. The trend inconsistency between land surface temperature and near surface air temperature in assessing urban heat island effects. Remote Sens 2020;12(8):1271.
[71] Norby RJ, Warren JM, Iversen CM, Childs J, Jawdy S, Walker AP. Forest stand and canopy development unaltered by 12 years of CO_2 enrichment. Tree Physiol 2021;42(3):428–40.
[72] Xu X, Yi C, Montagnani L, Kutter E. Numerical study of the interplay between thermo-topographic slope flow and synoptic flow on canopy transport processes. Agric For Meteorol 2018;255:3–16.
[73] Yang J, Liu P, Song H, Miao C, Wang F, Xing Y, et al. Effects of anthropogenic emissions from different sectors on $PM_{2.5}$ concentrations in Chinese cities. Int J Environ Res Public Health 2021;18(20):10869.
[74] Chun B, Guldmann JM. Spatial statistical analysis and simulation of the urban heat island in high-density central cities. Landsc Urban Plan 2014;125:76–88.
[75] Dirksen M, Ronda RJ, Theeuwes NE, Pagani GA. Sky view factor calculations and its application in urban heat island studies. Urban Clim 2019;30:100498.
[76] Cheung PK, Fung CK, Jim CY. Seasonal and meteorological effects on the cooling magnitude of trees in subtropical climate. Build Environ 2020;177:106911.
[77] Jin H, Liu S, Kang J. Thermal comfort range and influence factor of urban pedestrian streets in severe cold regions. Energ Buildings 2019;198:197–206.
[78] King G, Roland-Mieszkowski M, Jason T, Rainham DG. Noise levels associated with urban land use. J Urban Health 2012;89:1017–30.
[79] McAlexander TP, Gershon RR, Neitzel RL. Street-level noise in an urban setting: assessment and contribution to personal exposure. Environ Health 2015;14:1–10.
[80] Alam MS, Corcoran L, King EA, McNabola A, Pilla F. Modelling of intra-urban variability of prevailing ambient noise at different temporal resolution. Noise Mapp 2017;4(1):20–44.
[81] Lin H, Li Y, Zhao L. Partitioning of sensible and latent heat fluxes in different vegetation types and their spatiotemporal variations based on 203 FLUXNET sites. J Geophys Res-Atmos 2022;127(21):e2022JD037142.
[82] Santamouris M. Cooling the cities—a review of reflective and green roof mitigation technologies to fight heat island and improve comfort in urban environments. Sol Energy 2014;103:682–703.
[83] Han Q, Nan X, Wang H, Hu Y, Bao Z, Yan H. Optimizing the surrounding building configuration to improve the cooling ability of urban parks on surrounding neighborhoods. Atmosphere 2023;14(6):914.
[84] Potchter O, Cohen P, Bitan A. Climatic behavior of various urban parks during hot and humid summer in the Mediterranean city of Tel Aviv, Israel. Int J Climatol 2006;26(12):1695–711.
[85] Cheung PK, Jim CY, Siu CT. Effects of urban park design features on summer air temperature and humidity in compact-city milieu. Appl Geogr 2021;129:102439.
[86] Pioppi B, Pisello AL, Ramamurthy P. Wearable sensing techniques to understand pedestrian-level outdoor microclimate affecting heat related risk in urban parks. Sol Energy 2022;242:397–412.
[87] Wang L, Chen S, Chen L, Wang Z, Liu B, Xu Y. A new urban built-up index and its application in national central cities of China. ISPRS Int J Geo Inf 2024;13(1):21.
[88] Yan H, Wu F, Dong L. Influence of a large urban park on the local urban thermal environment. Sci Total Environ 2018;622:882–91.
[89] Sahani J, Biswal A, Dwivedi AK, Khalili S, Sun H, Andrade MF, et al. Quantifying the co-benefits of a tropical urban park in São Paulo through integrated mobile and stationary monitoring. City Environ Interact 2026;30:100360.
[90] Oke TR, Mills G, Christen A, Voogt JA. Urban climates. Cambridge University Press; 2017.
[91] Morakinyo TE, Lau KKL, Ren C, Ng E. Performance of Hong Kong's common trees species for outdoor temperature regulation, thermal comfort and energy saving. Build Environ 2018;137:157–70.
[92] Abdallah ASH, Hussein SW, Nayel M. The impact of outdoor shading strategies on student thermal comfort in open spaces between education building. Sustain Cities Soc 2020;58:102124.
[93] Wang R, Liu R, Chen Q, Cheng Q, Du M. Effects of sky view factor on thermal environment in different local climate zoning building scenarios—a case study of Beijing, China. Buildings 2023;13(8):1882.
[94] Khamchiangta D, Dhakal S. Physical and non-physical factors driving urban heat island: case of Bangkok Metropolitan Administration, Thailand. J Environ Manage 2019;248:109285.
[95] Ogce S, Ogce H, Yu S, Brown RD. The interaction between urban heat island and urban parks: An in-situ measurement-based review. Land Use Policy 2025;157: 107628.
[96] Skoulika F, Santamouris M, Kolokotsa D, Boemi N. On the thermal characteristics and the mitigation potential of a medium size urban park in Athens, Greece. Landsc Urban Plan 2014;123:73–86.
[97] Ramamurthy P, Bou-Zeid E. Heatwaves and urban heat islands: a comparative analysis of multiple cities. J Geophys Res-Atmos 2017;122:168–78.
[98] Norouzi M, Chau HW, Jamei E. Design and site-related factors impacting the cooling performance of urban parks in different climate zones: a systematic review. Land 2024;13(12):2175.
[99] Paz D, de Andrés JM, Narros A, Silibello C, Finardi S, Fares S, et al. Assessment of air quality and meteorological changes induced by future vegetation in Madrid. Forests 2022;13:690.
[100] Mahdavinejad M, Salehnejad H, Moradi N. An ENVI-met simulation study on influence of urban vegetation congestion on pollution dispersion. Asian Journal of Water, Environment and Pollution 2018;15(2):187–94.
[101] Qi Q, Meng Q, Wang J, He B, Liang H, Ren P. Applicability of mobile-measurement strategies to different periods: a field campaign in a precinct with a block park. Build Environ 2022;211:108762.
[102] Doick KJ, Peace A, Hutchings TR. The role of one large greenspace in mitigating London's nocturnal urban heat island. Sci Total Environ 2014;493:662–71.
[103] Geng X, Yu Z, Zhang D, Li C, Yuan Y, Wang X. The influence of local background climate on the dominant factors and threshold-size of the cooling effect of urban parks. Sci Total Environ 2022;823:153806.
[104] Liu Z, Fu L, Wu C, Zhang Z, Zhang Z, Lin X, et al. Spatialized importance of key factors affecting park cooling intensity based on the park scale. Sustain Cities Soc 2023;99:104952.
[105] Yu S, Chen Z, Yu B, Wang L, Wu B, Wu J, et al. Exploring the relationship between 2D/3D landscape pattern and land surface temperature based on explainable eXtreme Gradient Boosting tree: a case study of Shanghai, China. Sci Total Environ 2020;725:138229.
[106] Kusuma ASW, Rudiarto I, Mussadun M. Analysis of the need for Green Open Space (RTH) as an absorptor of carbondioxide gas emissions in the Semarang-Yogyakarta National road corridor, Bergas District, Semarang Regency. Eduvest J Univ Stud 2023;3(10):1776–88.
[107] Liu D, Lei L, Guo L, Zeng ZC. A cluster of CO2 change characteristics with GOSAT observations for viewing the spatial pattern of CO2 emission and absorption. Atmosphere 2015;6(11):1695–713.

[108] Pospisil J, Huzlik J, Licbinsky R, Spilacek M. Dispersion characteristics of PM10 particles identified by numerical simulation in the vicinity of roads passing through various types of urban areas. Atmosphere 2020;11(5):454.
[109] Patel J, Katapally TR, Khadilkar A, Bhawra J. The interplay between air pollution, built environment, and physical activity: perceptions of children and youth in rural and urban India. Health Place 2024;85:103167.
[110] Chen L, Liu C, Zou R, Yang M, Zahng Z. Experimental examination of effectiveness of vegetation as bio-filter of particulate matters in the urban environment. Environ Pollut 2016;208:198–208.
[111] Kumar P, Fennell P, Britter R. Effect of wind direction and speed on the dispersion of nucleation and accumulation mode particles in an urban street canyon. Sci Total Environ 2008;402:82–94.
[112] Brantley HL, Hagler GS, Deshmukh PJ, Baldauf RW. Field assessment of the effects of roadside vegetation on near-road black carbon and particulate matter. Sci Total Environ 2014;468:120–9.
[113] Rui L, Buccolieri R, Gao Z, Ding W, Shen J. The impact of green space layouts on microclimate and air quality in residential districts of Nanjing, China. Forests 2018;9(4):224.
[114] Janhäll S. Review on urban vegetation and particle air pollution–deposition and dispersion. Atmos Environ 2015;105:130–7.
[115] Abhijith KV, Kumar P, Gallagher J, McNabola A, Baldauf R, Pilla F, et al. Air pollution abatement performances of green infrastructure in open road and built-up street canyon environments – a review. Atmos Environ 2017;162:71–86.
[116] Bohatkiewicz J, Hałucha M, Dębiński MK, Jukowski M, Tabor Z. Investigation of acoustic properties of different types of low-noise road surfacers under in situ and laboratory conditions. Materials 2022;15(2):480.
[117] Fletcher DH, Garrett JK, Thomas A, Fitch A, Cryle P, Shilton S, et al. Location, location, location: modelling of noise mitigation by Urban Woodland shows the benefit of targeted tree planting in cities. Sustainability 2022;14:7079.
[118] Jaszczak A, Małkowska N, Kristianova K, Bernat S, Pochodyła E. Evaluation of soundscapes in urban parks in olsztyn (Poland) for improvement of landscape design and management. Land 2021;10(1):66.
[119] Sztubecka M, Skiba M, Mrówczyńska M, Mathias M. Noise as a factor of green areas soundscape creation. Sustainability 2020;12(3):999.
[120] AlSaleem SS, Almhafdy A, Berardi U, Al-Shargabi AA, Ali AAM. Field measurements and human perception to remediate noise pollution in the Urban Public Parks in Saudi Arabia. Sustainability 2023;15(13):9977.
[121] Xu C, Han B, Lu F, Wu T. Assessing the traffic noise reduction effect of roadside green space using LiDAR point cloud data in Shenzhen, China. Forests 2022;13 (5):765.
[122] Margaritis E, Kang J. Relationship between green space-related morphology and noise pollution. Ecol Indic 2017;72:477–89.
[123] Van Renterghem T, Botteldooren D, Verheyen G. Road traffic noise shielding by vegetation belts of limited depth. J Sound Vib 2012;331(10):2435–57.
[124] Demuzere M, Orru K, Heidrich O, Olazabal E, Geneletti D, Faehnle M, et al. Mitigating and adapting to climate change: multi-functional and multi-scale assessment of green urban infrastructure. J Environ Manag 2014;146:107–15.
[125] Kumar P, Druckman A, Gallagher J, Gatersleben B, Allison S, Eisenman TS, et al. The nexus between air pollution, green infrastructure and human health. Environ Int 2019;133:105181.
[126] Birenboim A, Helbich M, Kwan M. Advances in portable sensing for urban environments: understanding cities from a mobility perspective. Comput Environ Urban Syst 2021;88:101650.
[127] Ferrini F, Fini A, Mori J, Gori A. Role of vegetation as a mitigating factor in the urban context. Sustainability 2020;12(10):4247.
[128] Yao J, Jia X, Liao Z. Exploring the impact of nocturnal boundary layer stability on wintertime air pollution in a highly polluted basin city using unsupervised learning classification. Atmos Pollut Res 2024;15(10):102253.
[129] Li L, Xu Z, Zhou S. Research progress in micro-scale environmental monitoring, exposure and individual response in Chinese literature. Trans Urban Data Sci Technol 2024;3:121–35.